

Wakefield Acceleration in Nanostructures

Workshop on beam
acceleration in crystals and
nanostructures
and
Fermilab Colloquium
June 25, 2019

Toshi Tajima
UC Irvine

In dedication to the late Prof. Gaurang Yodh:
The last student of Enrico Fermi, at U. Chicago (PhD. 1955), passed away June 3, 2019

collaboration: G. Mourou, K. Nakajima, S. Hakimi, S. Bulanov, T. Ebisuzaki, X. Yan, M. Zhou, A. Chao, K. Abazajian, X. M. Zhang, D. Farinella, P. Taborek, F. Dollar, J. Wheeler, Y.M. Shin, V. Shiltsev, N. Naumova, W. J. Sha, J. C. Chanteloup, S. Nicks, D. Roa, A. Necas, C. Barty

- Introduction
- Fiber **laser** and ascent toward 100GeV and collider (and a tiny **laser**)
- Single-cycled **laser** and “TeV on a chip”
- Nature’s favorite acceleration:
cosmic wakefield
- Accelerator to our body

Fermi PeV Accelerator

$$\alpha = \frac{e^2}{\hbar c}$$

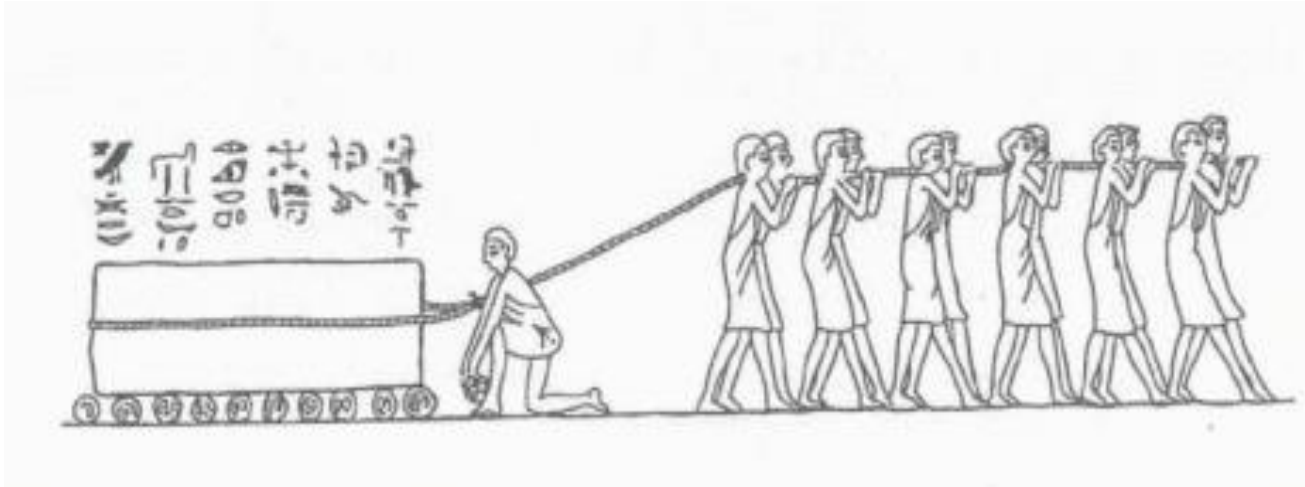


Also, Fermi's cosmic acceleration (1954): stochastic acceleration

Plasma accelerator driven by beam/pulse

Collective force $\sim N^2$ (nonlinear ← linear force $\sim N$)

Coherent and smooth structure (not stochastic)



Plasma accelerator driven by **laser** (coherent photons)

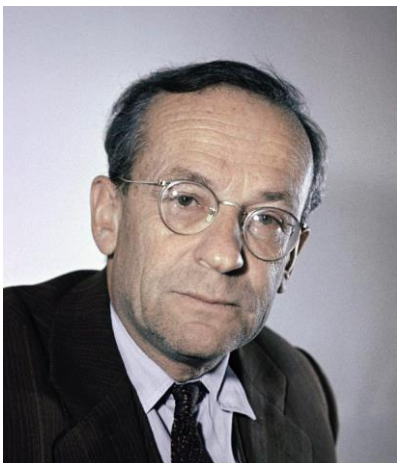
← [*Fermi*'s challenge for PeV accelerator]

compactification by $10^3 - 10^4$ (even by 10^6) >> conventional accelerators

enabled by **laser** technology (intense ultrafast **laser compression** (Mourou et al. 1985, 2013))

[particle beam-driven case: similar (if a bit lower)]

Acceleration by plasma **wake** waves: History



V. Veksler



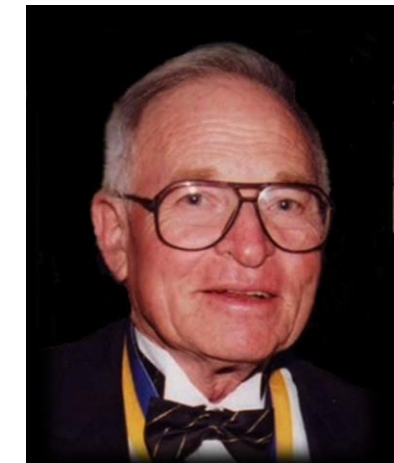
J. Dawson

Collective acceleration suggested:

Veksler (1956, CERN)

Driven by electron beam

(ion energy)~(M/m)(electron energy)



N. Rostoker

Many experimental attempts

of plasma acceleration (~60's -'70s,

Rostoker's lab UCI included)

led to no such amplification

(ion energy)~(2 α +1)x(electron) **Mako-Tajima (UCI) analysis** (1978;1984)

sudden acceleration, ions untrapped,
electrons return, while some run away
→ #1 **gradual acceleration necessary**

→ **Tajima-Dawson (1979, UCLA) wakefield**

#2 **electron acceleration** possible

with **trapping (with the Tajima-**

Dawson field) with **laser**, **more tolerant** for
sudden process

Target Normal Sheath Acceleration

laser-driven ion acceleration (LLNL,2000)
sudden acceleration, ions untrapped

Laser Wakefield (LWFA):

Wake phase velocity \gg water movement speed
maintains **coherent** and **smooth** structure



vs

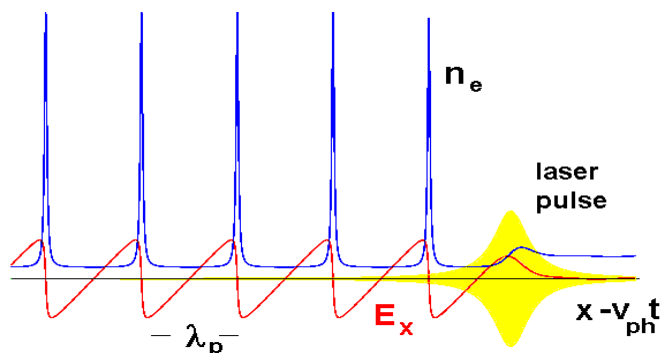
Tsunami phase velocity becomes ~ 0 ,
causes **wavebreak** and **turbulence**



Strong beam (of **laser** / particles) drives plasma waves to saturation amplitude: $E = m\omega_{ph}v_{ph}/e$

No wave breaks and wake **peaks** at $v \approx c$

Wave **breaks** at $v < c$

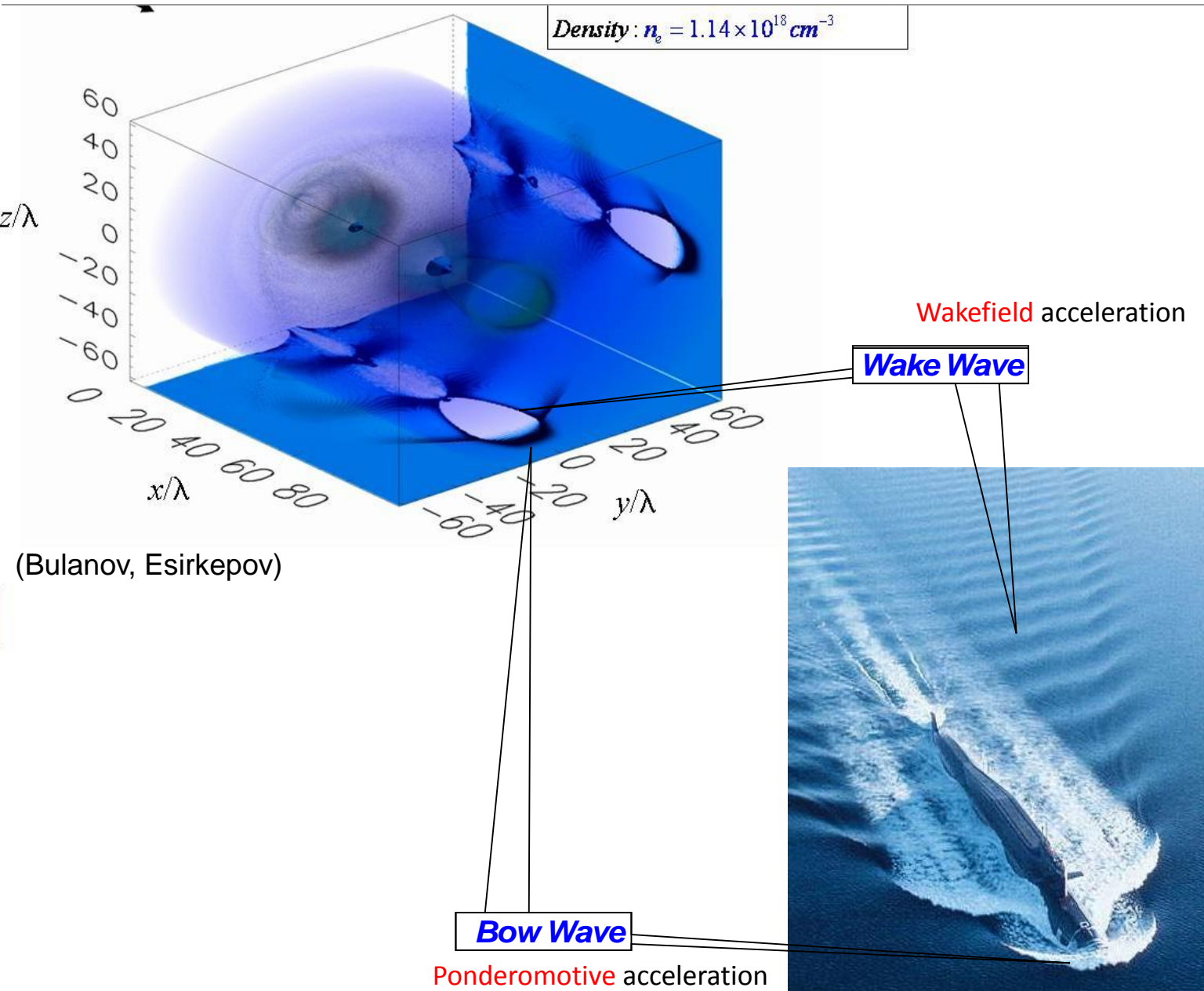


← relativity
regularizes
(*relativistic coherence*)



Relativistic coherence enhances beyond the Tajima-Dawson field $E = m\omega_p c/e$ (\sim GeV/cm)

Laser-driven Bow and Wake



The late Prof. Abdus Salam



At ICTP Summer School (1981),
Prof. Salam summoned me and discussed
about **laser wakefield** acceleration.

Salam: '*Scientists like me began feeling
that we had less means to test our theory.
However, with your laser acceleration,
I am encouraged*'. (1981)

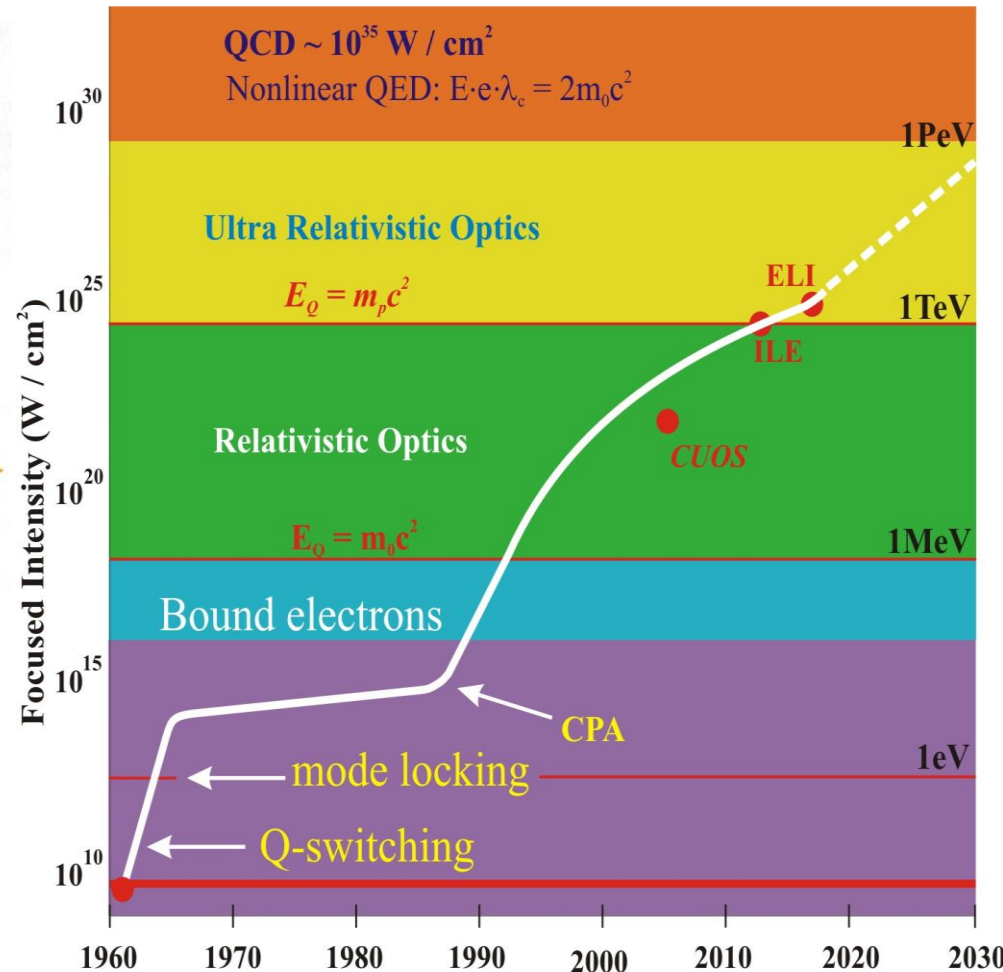
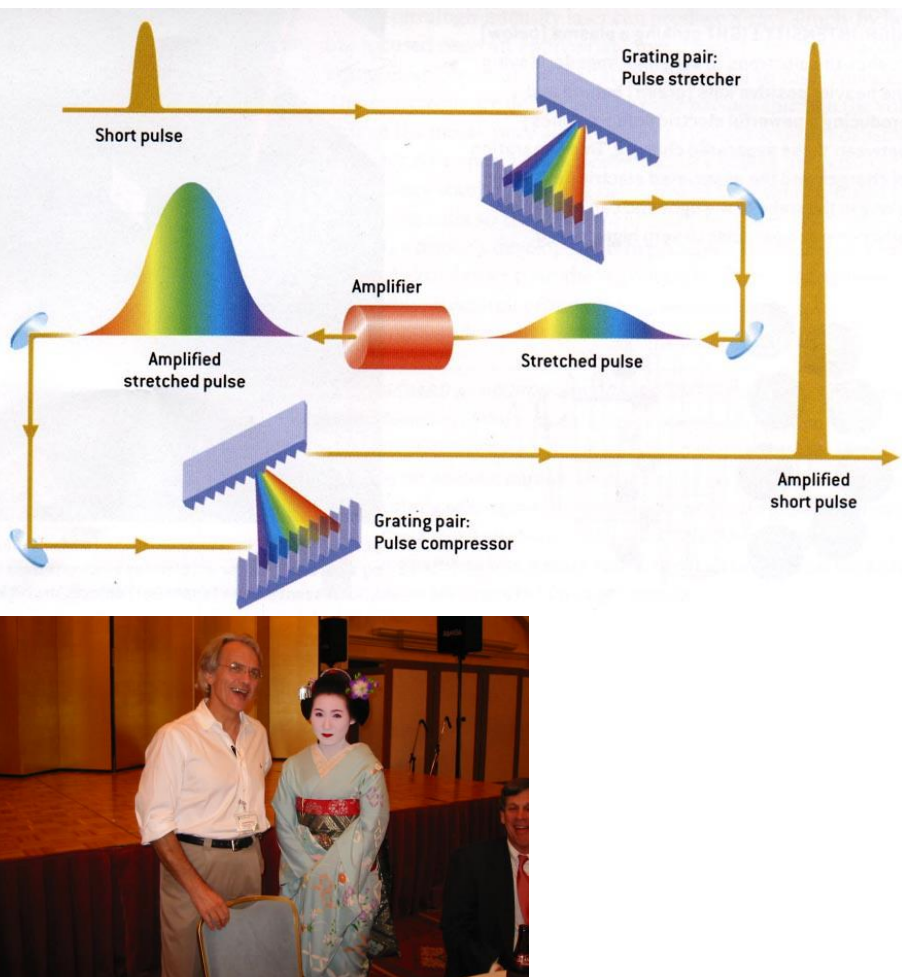
He organized the Oxford Workshop
on **laser wakefield** accelerator in 1982.

Effort: many scientists over many years to realize his vision / dream
High field science: spawned

Ascent toward 100GeV and collier



Enabling technology: laser revolution

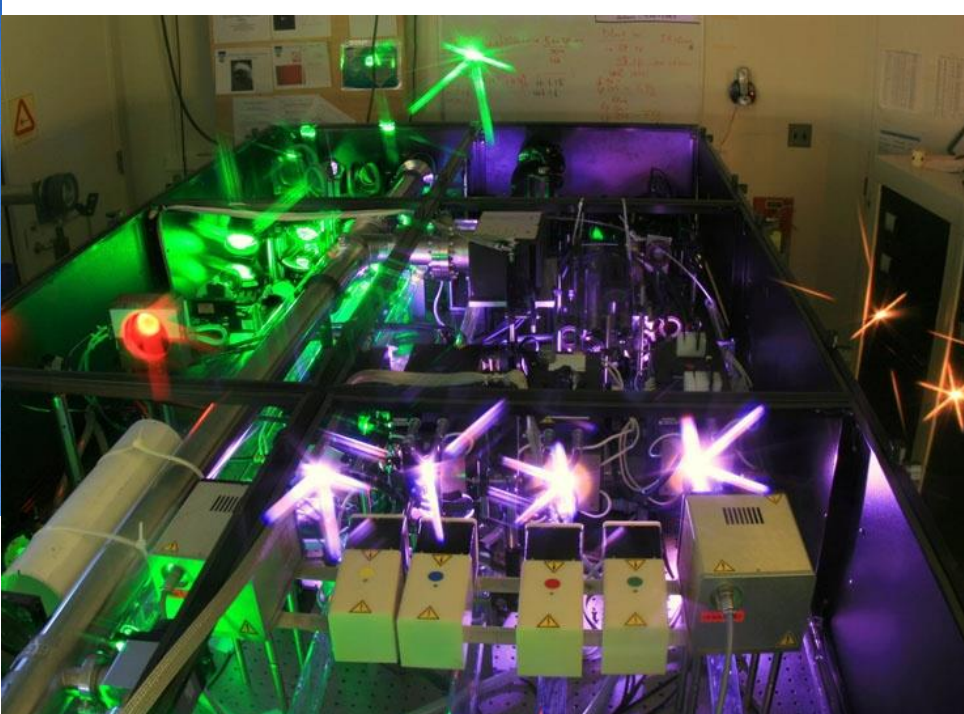


G. Mourou invented Chirped Pulse Amplification (1985)

Laser intensity exponentiated since,

to match the required intensity for Tajima-Dawson's LWFA (1979)

Demonstration, realization, and applications of laser wakefield accelerators



(Michigan)



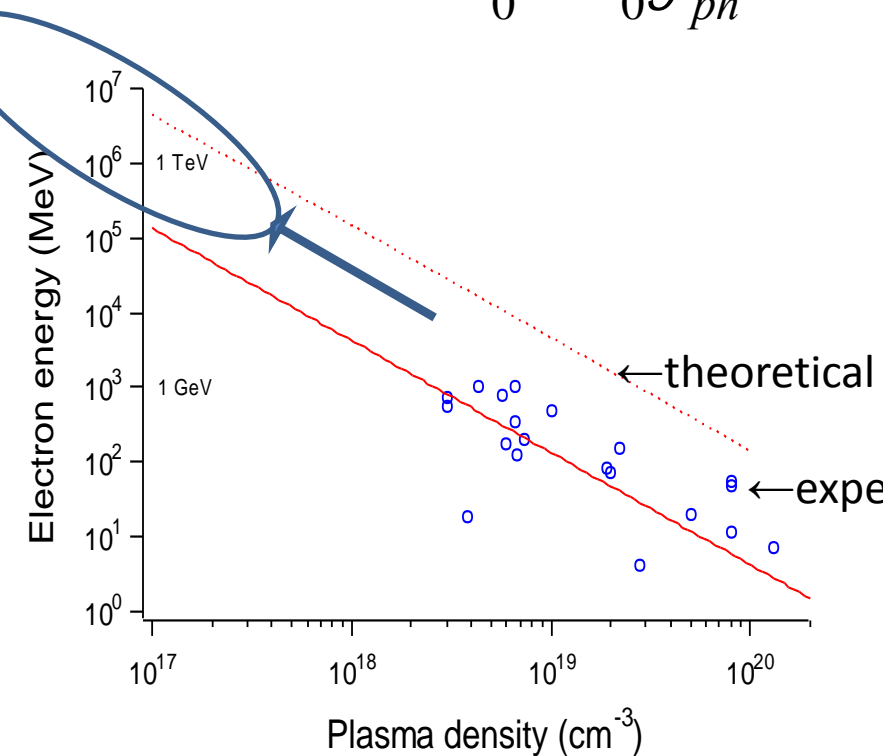
4 GeV laser accelerator LBL



3GeV Synchrotron SOLEIL



Theory of wakefield toward extreme energy



$$\Delta E \approx 2m_0c^2a_0^2g_{ph}^2 = 2m_0c^2a_0^2\left(\frac{n_{cr}}{n_e}\right), \quad (\text{when 1D theory applies})$$

In order to avoid wavebreak,

$$a_0 < \gamma_{ph}^{1/2},$$

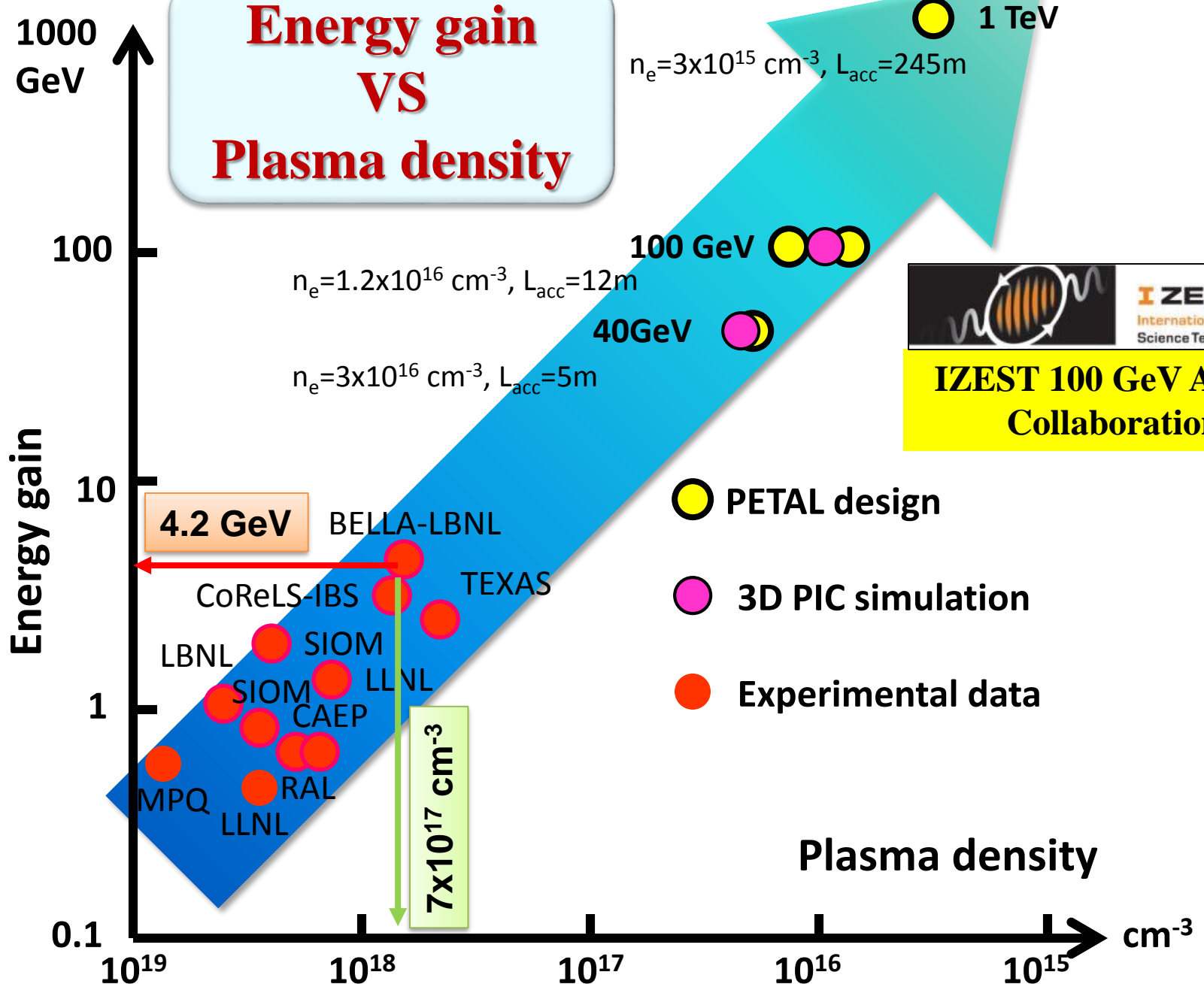
where

$$\gamma_{ph} = (n_{cr}/n_e)^{1/2}$$

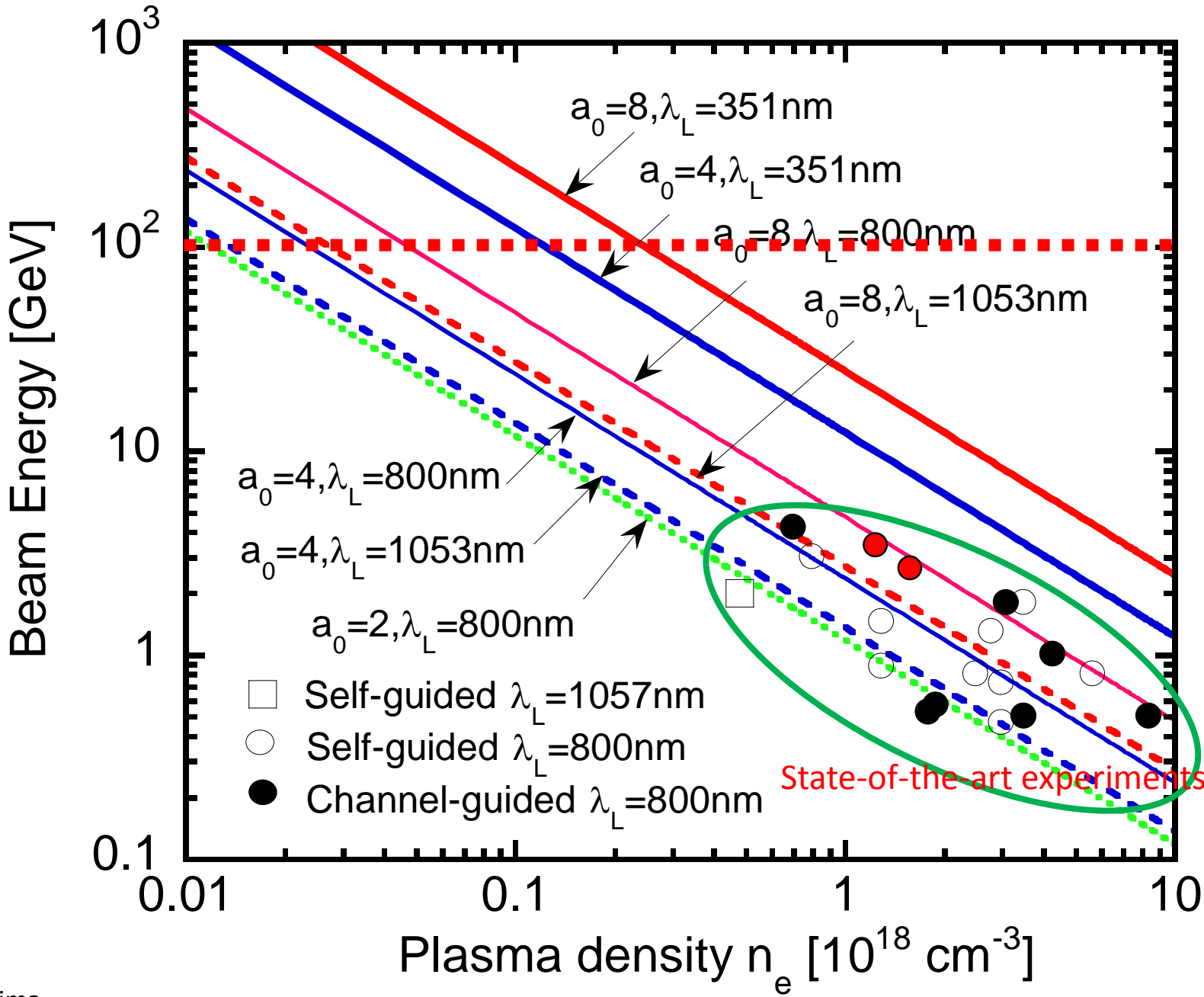
$$n_{cr} = 10^{21} \text{ (1eV photon)}$$

→ 10^{29} (10keV photon)

$$n_e = 10^{16} \text{ (gas)} \rightarrow 10^{23} \text{ (solid)}$$

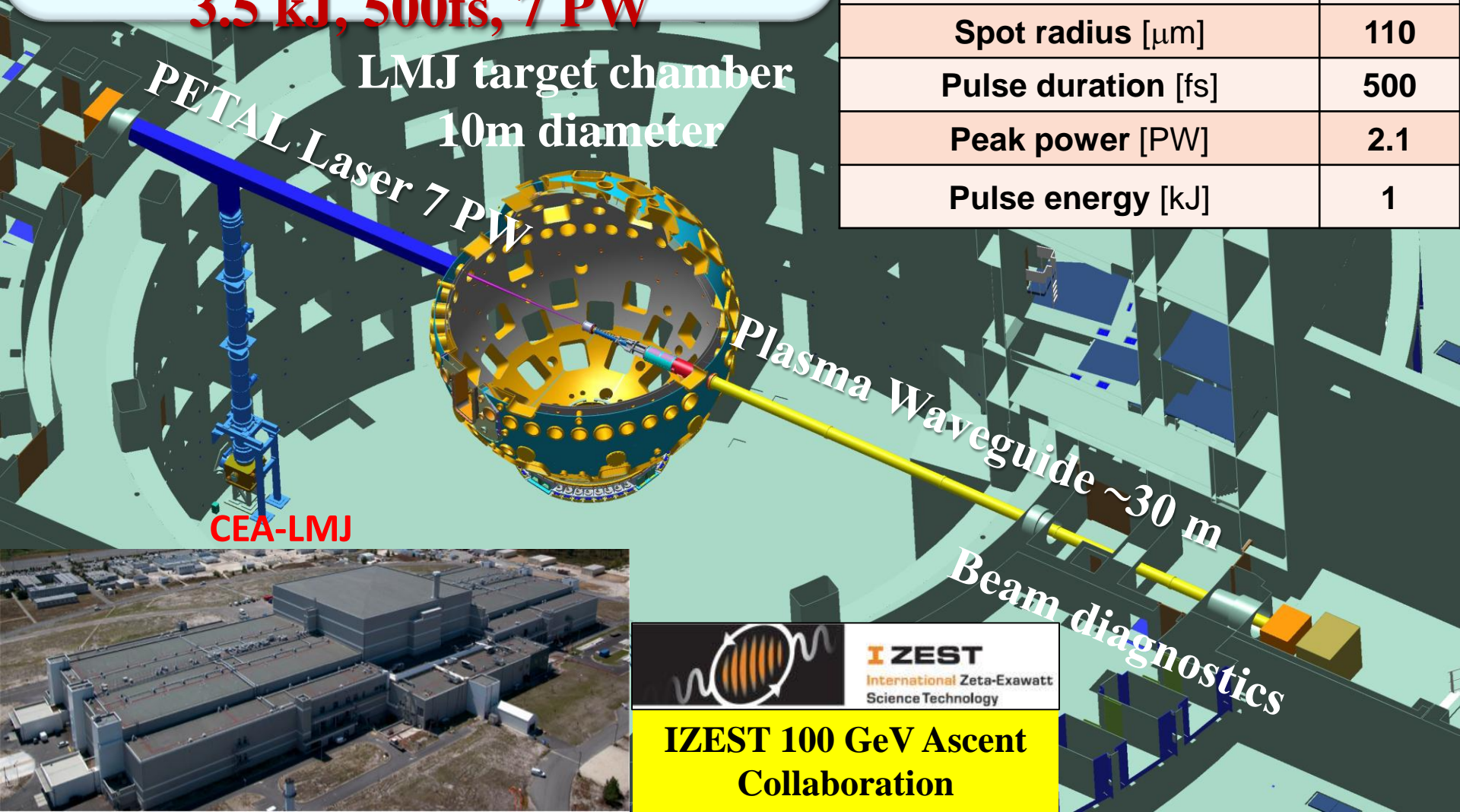


$1 \omega \rightarrow 3\omega$; 10times energy; 30times shorter



IZEST 100 GeV Ascent Plan

K. Nakajima
at CEA-Bordeaux
PETAL laser
3.5 kJ, 500fs, 7 PW



Experiment parameters

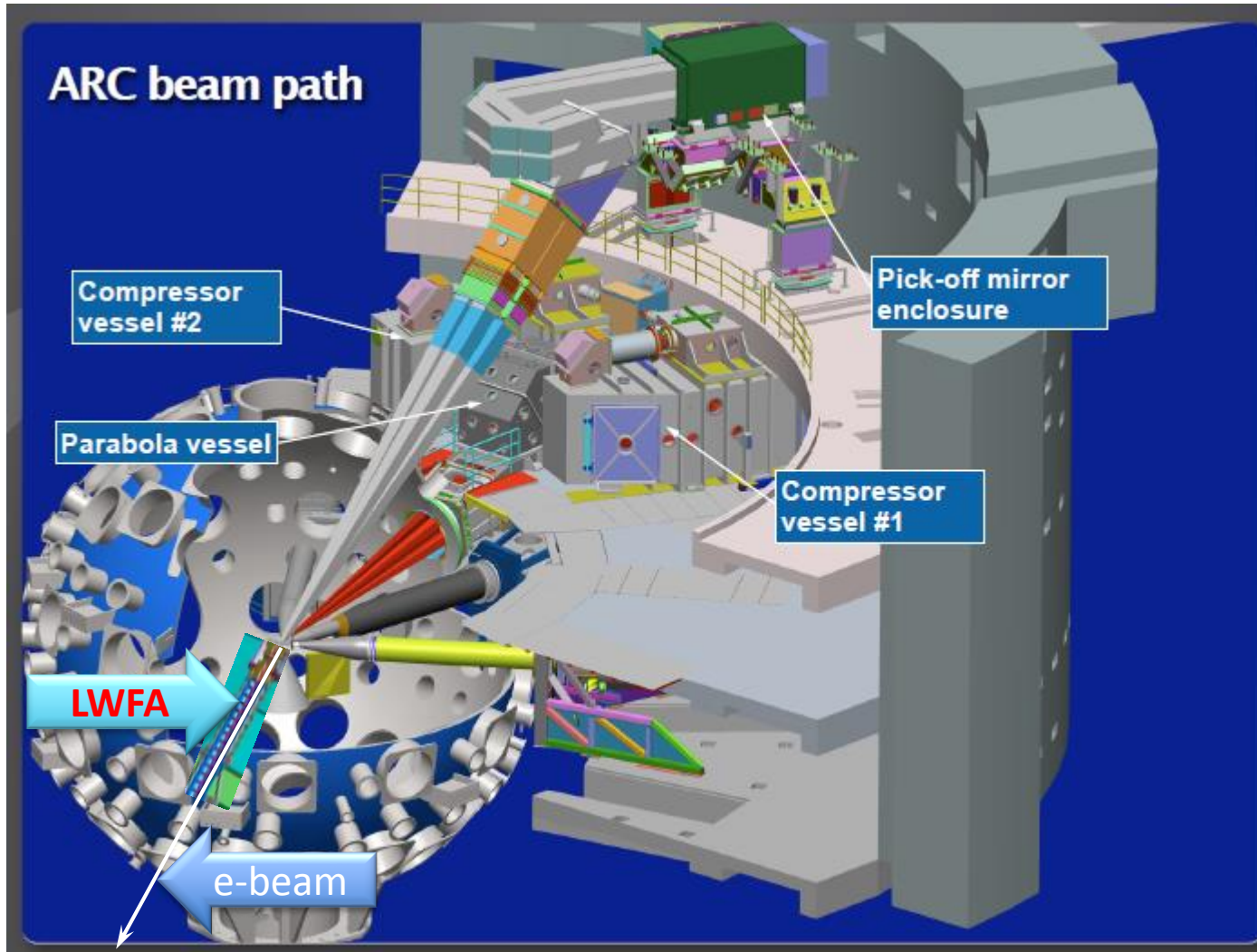
Energy gain [GeV]	100
Plasma density [10^{15} cm^{-3}]	12
Accelerator length [m]	12
Normalized field a_0	3
Spot radius [μm]	110
Pulse duration [fs]	500
Peak power [PW]	2.1
Pulse energy [kJ]	1

IZEST 100 GeV Ascent
Collaboration

I ZEST
International Zeta-Exawatt
Science Technology

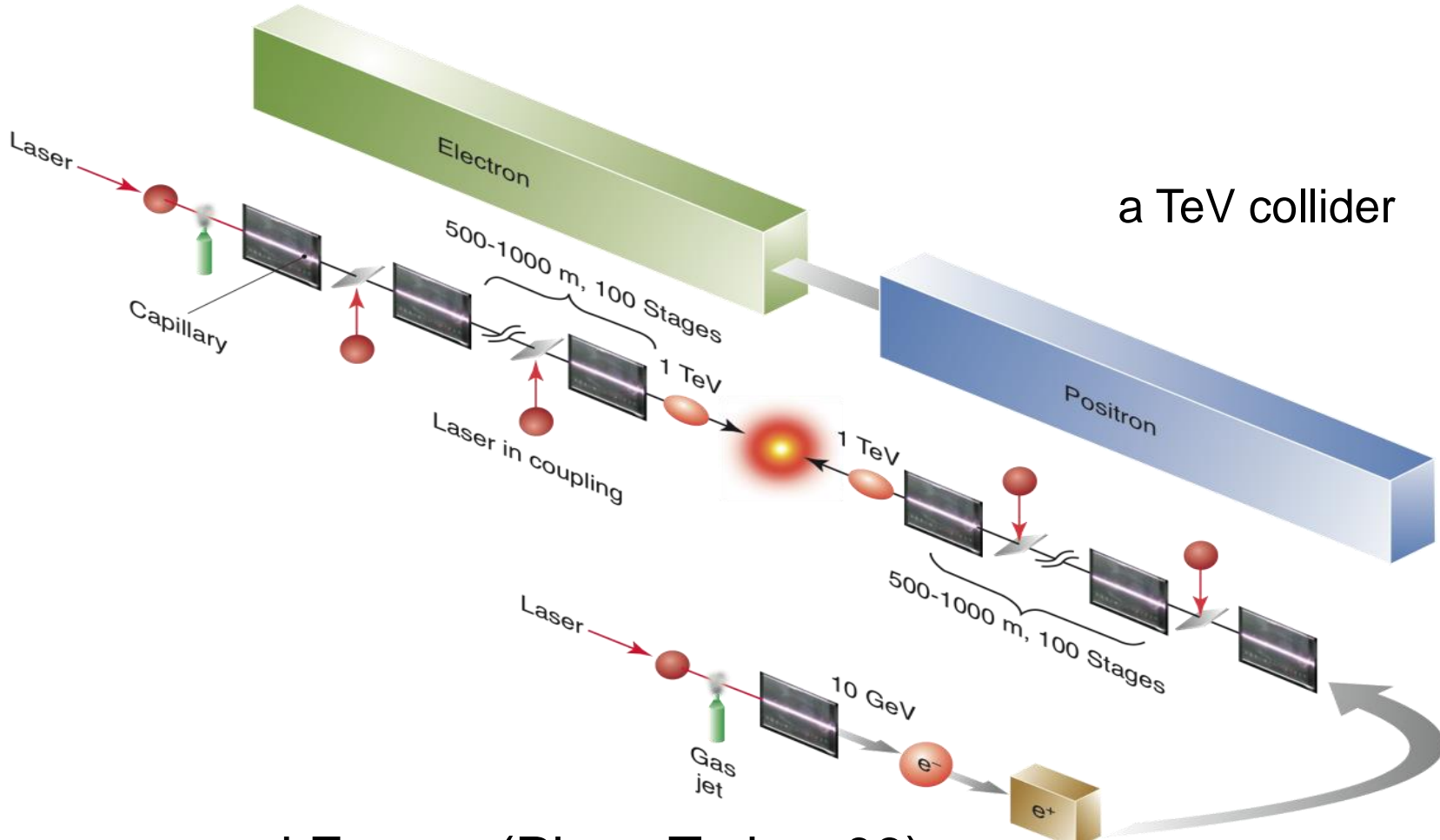


100 GeV UV LWFA experiment at ARC



by courtesy of C.P.J. Barty

Laser driven collider concept



Leemans and Esarey (Phys. Today, 09)

ICFA-ICUIL Joint Task Force on **Laser** Acceleration(Darmstadt,10)

for collider

Density scalings of **LWFA**

Accelerating field E_z	$\propto n_e^{1/2}$
Focusing constant K	$\propto n_e^{1/2}$
Stage length L_{stage}	$\propto n_e^{-3/2}$
Energy gain per stage W_{stage}	$\propto n_e^{-1}$
Number of stages N_{stage}	$\propto n_e$
Total linac length L_{total}	$\propto n_e^{-1/2}$
Number of particles per bunch N_b	$\propto n_e^{-1/2}$
Laser pulse duration τ_L	$\propto n_e^{-1/2}$
Laser peak power P_L	$\propto n_e^{-1}$
<u>Laser energy per stage U_L</u>	<u>$\propto n_e^{-3/2}$</u>
Radiation loss $\Delta\gamma$	$\propto n_e^{1/2}$
Radiative energy spread σ_γ/γ_f	$\propto n_e^{1/2}$
Initial normalized emittance ϵ_{n0}	$\propto n_e^{-1/2}$
Collision frequency f_c	$\propto n_e$
Beam power P_b	$\propto n_e^{1/2}$
Average laser power P_{avg}	$\propto n_e^{-1/2}$
<u>Wall plug power P_{wall}</u>	<u>$\propto n_e^{1/2}$</u>



ICFA-ICUIL Joint Task Force on laser acceleration (Darmstadt, 2010)



W. Leemans,
Chair

Collider subgroup
List of parameters
(W. Chou)

Table 1
Collider parameters

Case	1 TeV	10 TeV (Scenario I)	10 TeV (Scenario II)
Energy per beam (TeV)	0.5	5	5
Luminosity ($10^{34} \text{ cm}^{-2}\text{s}^{-1}$)	1.2	71.4	71.4
Electrons per bunch ($\times 10^9$)	4	4	1.3
Bunch repetition rate (kHz)	13	17	170
Horizontal emittance $\gamma\varepsilon_x$ (nm-rad)	700	200	200
Vertical emittance $\gamma\varepsilon_y$ (nm-rad)	700	200	200
β^* (mm)	0.2	0.2	0.2
Horizontal beam size at IP σ_x^* (nm)	12	2	2
Vertical beam size at IP σ_y^* (nm)	12	2	2
Luminosity enhancement factor	1.04	1.35	1.2
Bunch length σ_z (μm)	1	1	1
Beamstrahlung parameter Υ	148	8980	2800
Beamstrahlung photons per electron n_γ	1.68	3.67	2.4
Beamstrahlung energy loss δ_E (%)	30.4	48	32
Accelerating gradient (GV/m)	10	10	10
Average beam power (MW)	4.2	54	170
Wall plug to beam efficiency (%)	10	10	10
One linac length (km)	0.1	1.0	0.3



JTF Report #2



Case	1 TeV	10 TeV (Scenario I)	10 TeV (Scenario II)
Wavelength (μm)	1	1	1
Pulse energy/stage (J)	32	32	1
Pulse length (fs)	56	56	18
Repetition rate (kHz)	13	17	170
Peak power (TW)	240	240	24
Average laser power/stage (MW)	0.42	0.54	0.17
Energy gain/stage (GeV)	10	10	1
Stage length [LPA + in-coupling] (m)	2	2	0.06
Number of stages (one linac)	50	500	5000
Total laser power (MW)	42	540	1700
Total wall power (MW)	84	1080	3400
Laser to beam efficiency (%) [laser to wake 50% + wake to beam 40%]	20	20	20
Wall plug to laser efficiency (%)	50	50	50
Laser spot rms radius (μm)	69	69	22
Laser intensity (W/cm^2)	3×10^{18}	3×10^{18}	3×10^{18}
Laser strength parameter a_0	1.5	1.5	1.5
Plasma density (cm^{-3}), with tapering	10^{17}	10^{17}	10^{18}
Plasma wavelength (μm)	105	105	33

Collider subgroup
List of parameters
(W. Chou)

Table 2
Laser parameters



JTF Report #3: Comparison of Choices

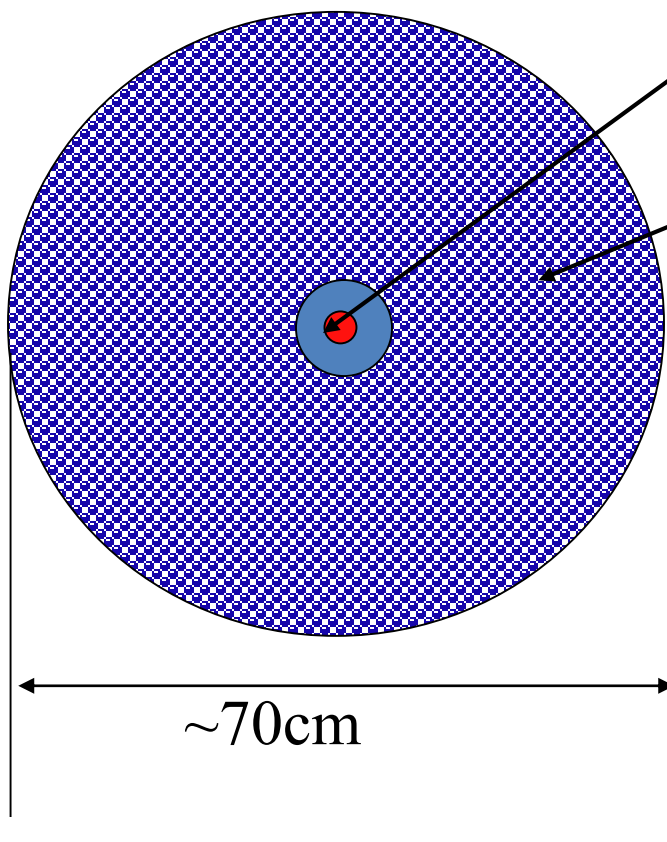


Accelerator	Beam	Beam energy (GeV)	Beam power (MW)	Efficiency AC to beam	Note on AC power
PSI Cyclotron	H ⁺	0.59	1.3	0.18	RF + magnets
SNS Linac	H ⁻	0.92	1.0	0.07	RF + cryo + cooling
TESLA (23.4 MV/m)	e ⁺ /e ⁻	250 × 2	23	0.24	RF + cryo + cooling
ILC (31.5 MV/m)	e ⁺ /e ⁻	250 × 2	21	0.16	RF + cryo + cooling
CLIC	e ⁺ /e ⁻	1500 × 2	29.4	0.09	RF + cooling
LPA	e ⁺ /e ⁻	500 × 2	8.4	0.10	Laser + plasma

CAN Laser:

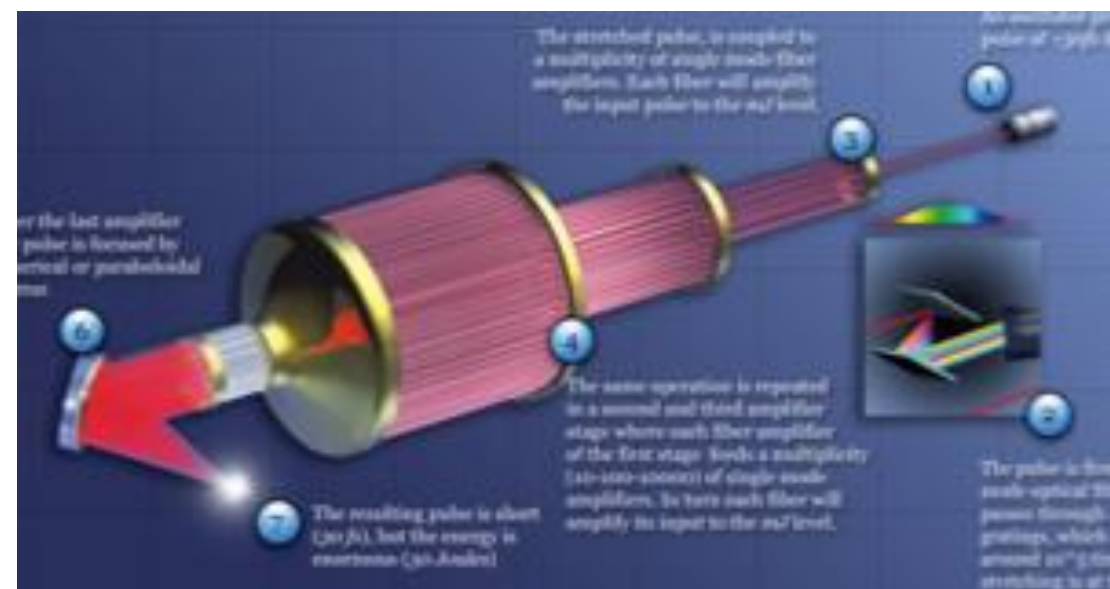
Need to Phase

32 J/1mJ/fiber~ 3×10^4 Phased Fibers!



Electron/positron beam

Transport fibers

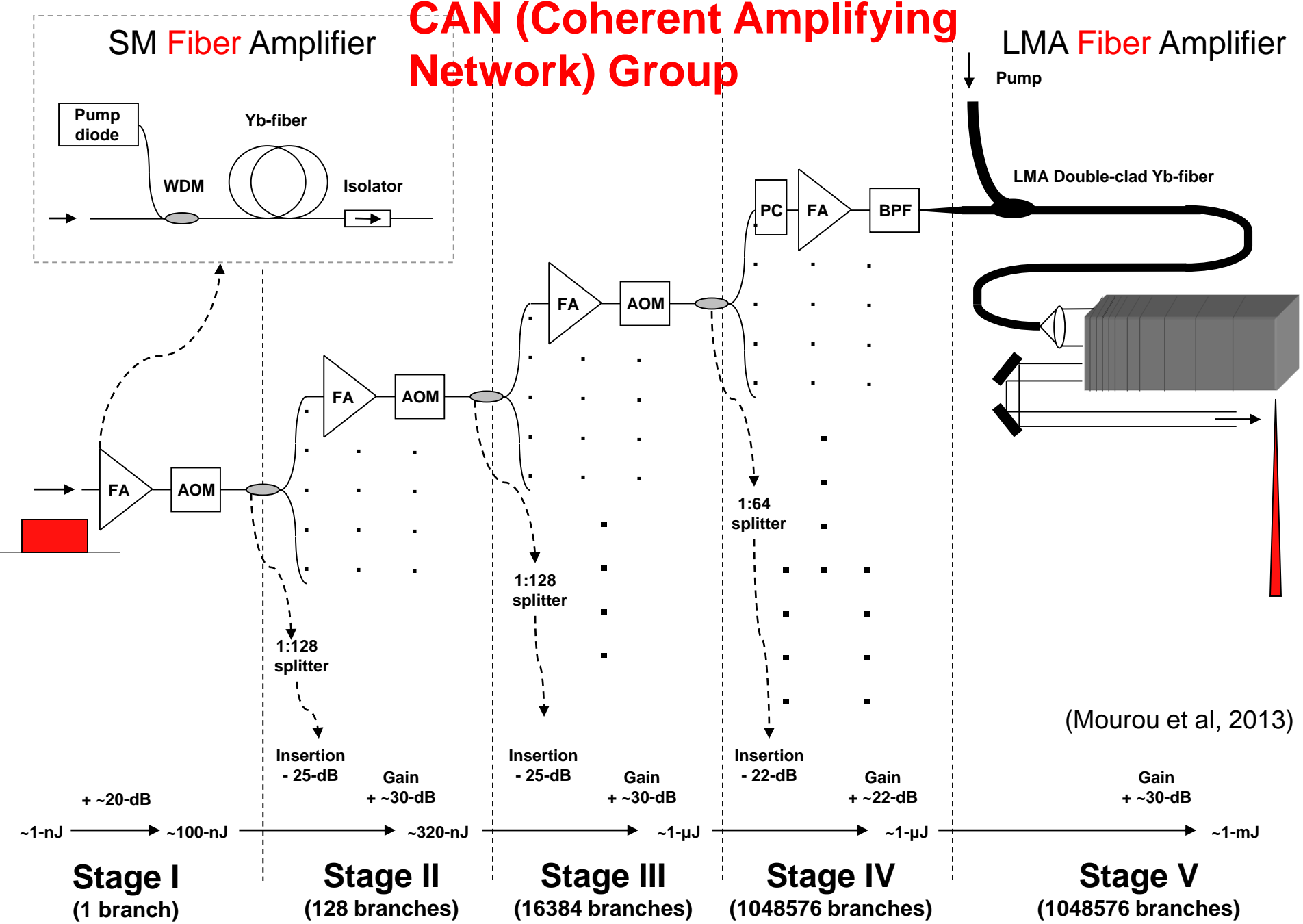


Length of a fiber ~2m

Total fiber length~ 5×10^4 km

G. Mourou: patent (2009)
Mourou, Brockesby, Tajima,
Limpert (2013)

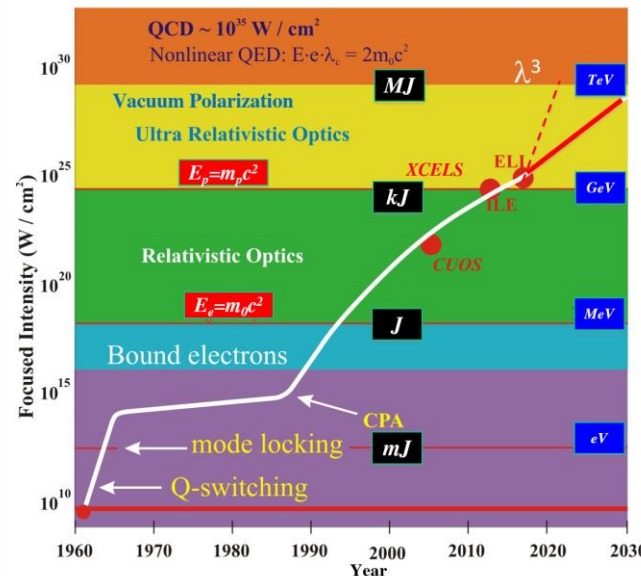
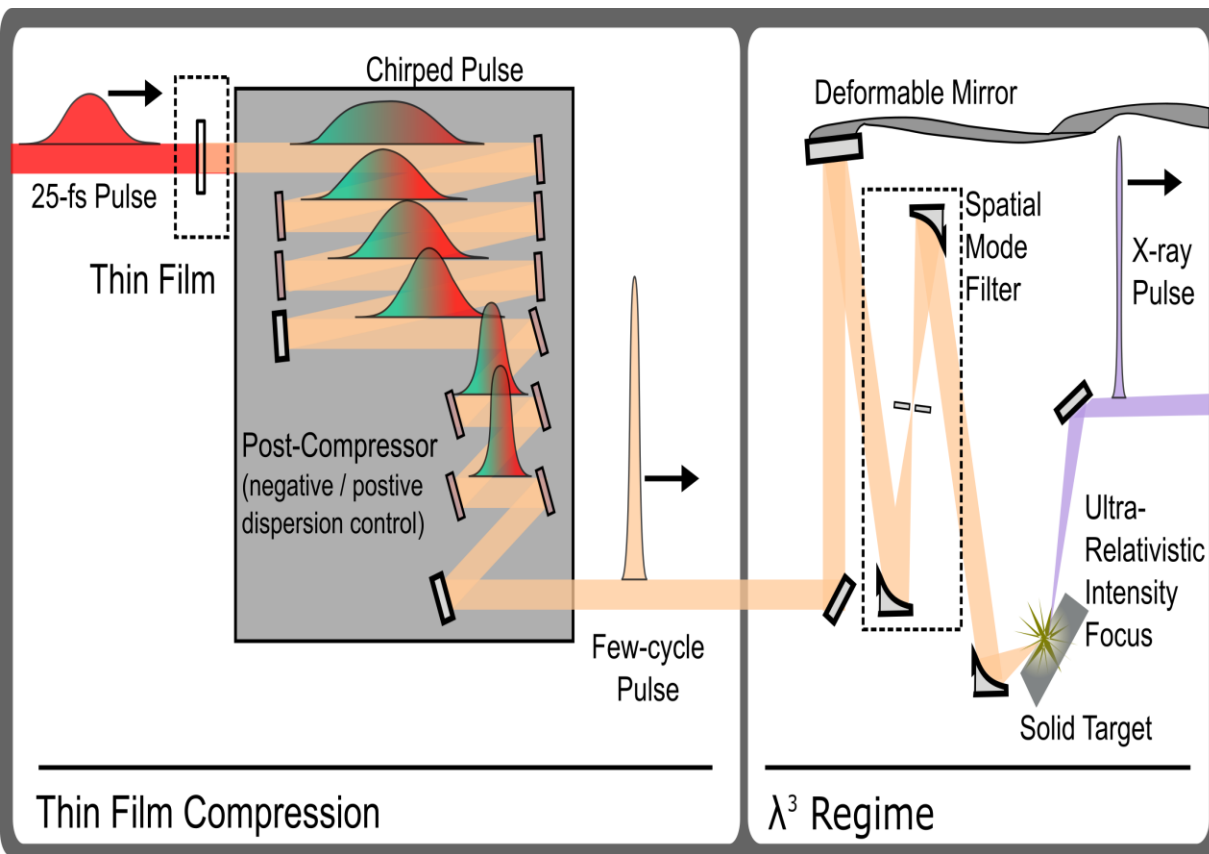
CAN (Coherent Amplifying Network) Group



Single-cycled **laser** and “TeV on a chip”



Thin film compression and single-cycle optical and X-ray lasers



X-ray LWFA in crystal suggested

X-ray Laser Wakefield Accelerator in crystal:

LWFA pump-depletion length:

$$L_{acc} \sim a_x (c/\omega_p) (\omega_x/\omega_p)^2, \quad (a_x = eE_x/mc\omega_x)$$

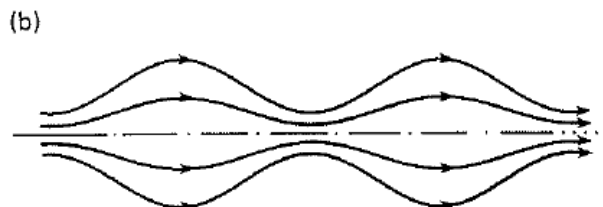
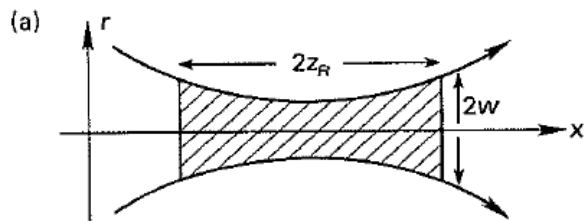
LWFA energy gain

$$\varepsilon_x = 2a_x^2 mc^2 (n_{cr}/n_e),$$

Here, $n_{cr} = 10^{29}$, $n_e = 10^{23}$, $a_x \sim 30$ (pancake laser pulse with the **Schwinger intensity**, with focal radius assumed the same as optical laser radius. Could be greater if we further focus by optics, or nonlinearity, or if we not limit the intensity **at** **Schwinger**. see below)

The **vacuum self-focus** power threshold

$$P_{cr} = (45/14) c E_S^2 \lambda^2 \alpha^{-1}, \quad (E_S : \text{Schwinger field})$$



Schwinger fiber acceleration in vacuum:

(no surface, no breakdown)

Vacuum photon dispersion relation with focus

$$\omega = c \sqrt{k_z^2 + \langle k_{perp}^2 \rangle},$$

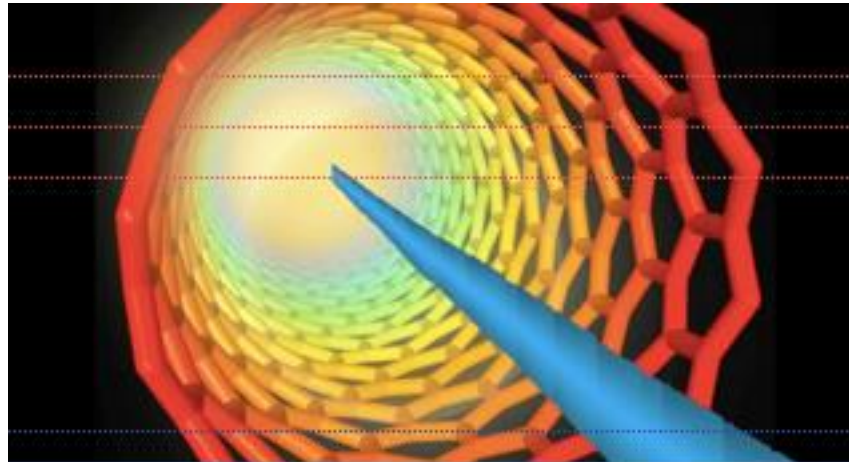
The **vacuum dispersion relation** with fiber self-modulation

$$\omega / (k_z + k_s) = c, \quad (k_s = 2\pi / s)$$

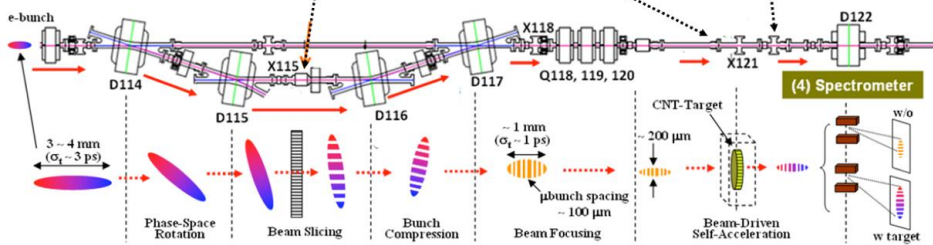
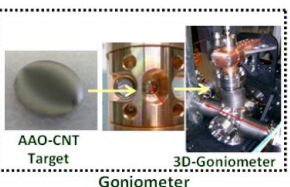
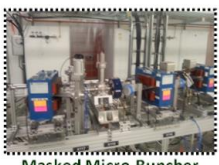
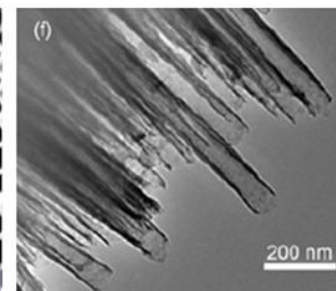
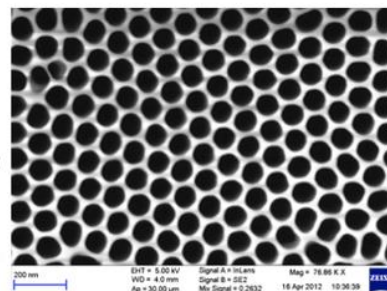
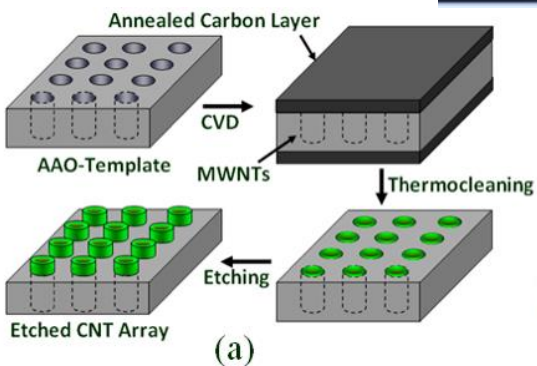
(Tajima and Cavenago, PRL, 1987)

Wakefield acceleration in porous nanomaterials

Carbon nanotube with
Particle beam / X-ray pulse



Porous nanomaterial



Collaboration (2015) with Fermilab / NIU
Y. Shin et al.

Earlier works of X-ray crystal acceleration

-X-ray optics and fields (Tajima et al. PRL, 1987)

-Nanocrystal hole for particle propagation (Newberger, Tajima, et al. 1989, AAC; PR,...)

-particle transport in the crystal (Tajima et al. 1990, PA)

APPLICATION OF NOVEL MATERIAL IN CRYSTAL ACCELERATOR CONCEPTS

B. Newberger, T. Tajima, The University of Texas at Austin, Austin, Texas 78712

F. R. Huson, W. Mackay, Texas Accelerator Center, The Woodlands, Texas

B. C. Covington, J. R. Payne, Z. G. Zou, Sam Houston State University, Huntsville, Texas

N. K. Mahale, S. Ohnuma, University of Houston, Houston, Texas 77004

which incorporate regular macroscopic features on the underlying crystal lattice are of potential application to crystal accelerators and coherent sources. We have recently begun an investigation of material, porous Si, in which pores of radii up to a lattice spacings are etched through finite volumes crystal. The potential reduction of losses to particles annealed along the pores makes this a very internal in crystal accelerators for relativistic, positively charges. Our results on material properties which are this context will be presented. The consequences transport will be discussed.

and $k = v_0/m_I c^2$, v_0 , is the “spring constant of the channel well. Its specific form depends on the model to construct the continuum potential of a string of atoms for purposes it suffices to take a typical value of 2×10^4 eV/nm². This is the multiple scattering velocity space “diffusion” We have used¹⁰

$$D = z\pi r_e^2 N Z_{\text{val}} \left(\frac{m_e}{m_I} \right)^2 L_R,$$

where r_e is the classical electron radius, Z_{val} is the number of valence electrons, and N is the number density of atoms. Logarithmic dependencies on particle energy are neglected throughout. L_R is a constant with a typical value of 10^{-10} nm.

Particle Accelerators, 1990, Vol. 32, pp. 235–240
Reprints available directly from the publisher
Photocopying permitted by license only

© 1990 Gordon and Breach, Science Publishers, Inc.
Printed in the United States of America

BEAM TRANSPORT IN THE CRYSTAL X-RAY ACCELERATOR

T. TAJIMA, B. S. NEWBERGER
University of Texas-Austin, Austin TX 78712 U.S.A.

F. R. HUSON, W. W. MACKAY
Texas Accelerator Center, The Woodlands, TX 77381 U.S.A.

B. C. COVINGTON, J. PAYNE
Sam Houston State University, Huntsville, TX 77341 U.S.A.

N. K. MAHALE, S. OHNUMA

University of Houston, Houston, TX 77204 U.S.A.

Abstract A Fokker-Planck model of charged particle transport in crystal channels which includes the effect of strong accelerating gradients has been developed¹ for application to

VOLUME 59, NUMBER 13

PHYSICAL REVIEW LETTERS

28 SEPTEMBER 1987

Crystal X-Ray Accelerator

T. Tajima

Department of Physics and Institute for Fusion Studies, The University of Texas, Austin, Texas 78712
and

M. Cavenago

Department of Physics, University of California, Irvine, California 92717
(Received 18 November 1986)

An ultimate linac structure is realized by an appropriate crystal lattice (superlattice) that serves as a “soft” iced waveguide for x rays. High-energy (≈ 40 keV) x rays are injected into the crystal at the Bragg angle to cause Bormann anomalous transmission, yielding slow-wave accelerating fields. Particles (e.g., muons) are accelerated along the crystal axis.

PACS numbers: 52.75.Di, 41.80.-y, 61.80.Mk

An approach to the attainment of ever higher energies by extrapolating the linac to higher accelerating fields, higher frequencies, and finer structures is prompted by several considerations, including the luminosity requirement which demands the radius of the colliding-beam spot to be proportionately small at high energies: $a_0 = \pi^{-1/2} \hbar c (f/N)^{-1/2} P_e^{-1/2}$, where f , N , P , and e are the duty cycle, total number of events, beam power, and beam energy, respectively. This approach, however, encounters a physical barrier when the photon energy becomes of the order $\hbar\omega = \hbar\omega_p = mc^2/a^2 = 30$ eV (a =the fine-structure constant), corresponding to wavelength (scale length) $\lambda = 500$ Å. The metallic wall begins to absorb the photon strongly, where ω_p is the plasma frequency corresponding to the crystal electron density. In addition, since the wall becomes not perfectly conducting for $\hbar\omega \geq mc^2/a^2$, the longitudinal component of fields becomes small and the photon goes almost straight into the wall (a soft-wall regime). As the photon energy $\hbar\omega$ much exceeds mc^2/a^2 and becomes $\gtrsim mc^2/a$, however, the metal now ceases to be opaque. The mean free path of the photon is given by Bethe-Bloch theory as $l_i = (3/2)^2 \pi \times a_B^{-2} a^{-1} n^{-1} (\hbar\omega/Z_{\text{eff}}^2 R)^{1/2}$, where a_B is the Bohr radius, n the electron density, Z_{eff} the effective charge of the lattice ion, and R the Rydberg energy.

In the present concept the photon energy is taken at the hard x-ray range of $\hbar\omega = mc^2/a$ and the linac structure is replaced by a crystal structure, e.g., silicon or GaAs-AlAs. (A similar bold endeavor was apparently undertaken by Hofstadter already in 1968.¹¹) Here the crystal axis provides the channel through which accelerated particles propagate with minimum scattering (channeling²) and the x rays are transmitted via the Bormann effect (anomalous transmission^{3,4}) when the x rays (wavelength λ) are injected in the xz plane with a polarization in their plane later converted to the yz plane.

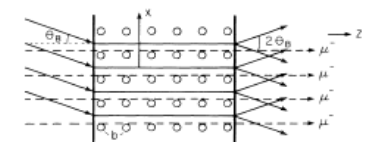
where b is the transverse lattice constant and later a the longitudinal lattice constant ($a=b$) (see Fig. 1). The row of lattice ions (perhaps with inner-shell electrons) constitutes the “waveguide” wall for x rays, while they also act as periodic irises to generate slow waves. A superlattice⁵ such as Ge_{1-x}S_x (in which the relative concentration x ranges from 0 to 1 over 100 Å or longer in the longitudinal z direction) brings in an additional freedom in the crystal structure and provides a small Brillouin wave number $k_x = 2\pi/s$ with s being the periodicity length. We demand that the x-ray light in the crystal channel walls becomes a slow wave and satisfies the high-energy acceleration condition

$$\omega/(k_z + k_s) = c, \quad (2)$$

where ω and k_z are the light frequency and longitudinal wave number.

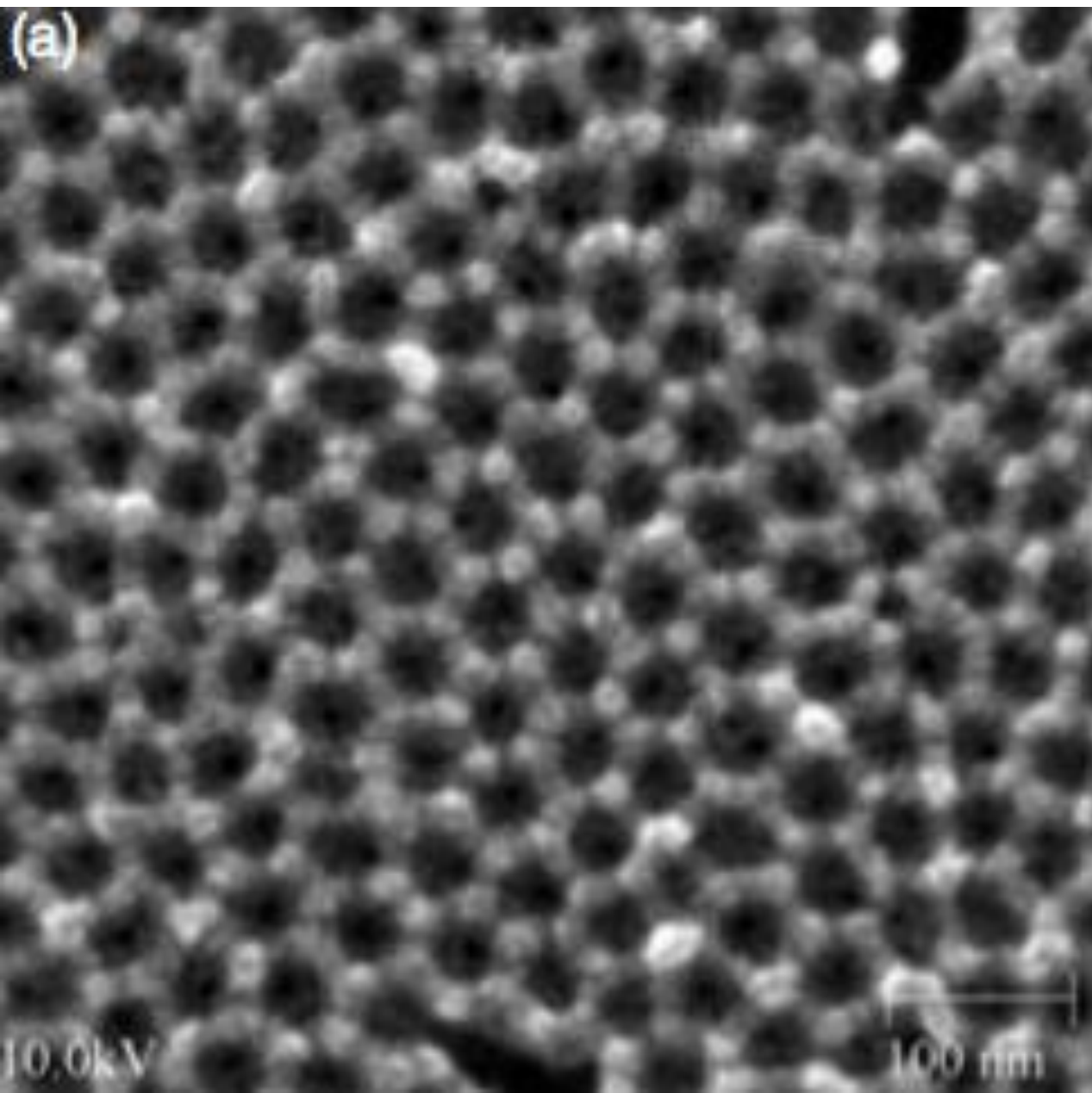
The energy loss of moving particles in matter is due to ionization, bremsstrahlung, and nuclear collisions. We can show⁶ that a channeled high-energy particle moving fast in the z direction oscillates in the xy plane according to the Hamiltonian

$$H = \frac{1}{2m} (\rho_x^2 + \rho_y^2) + V(x, y), \quad (3)$$



Porous Nanomaterial

(a)

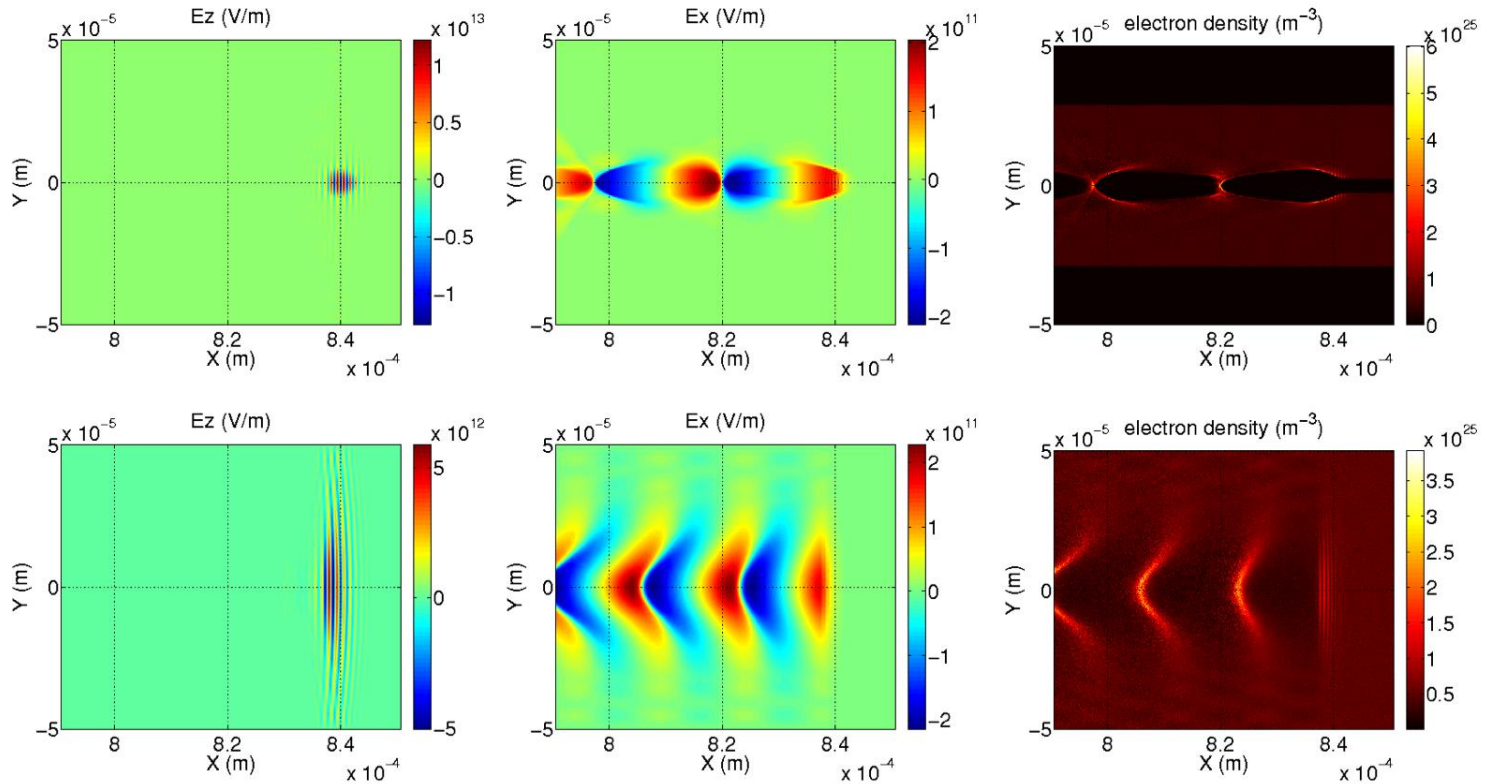


10.0 kV

100 nm

Porous alimina on Si substrate
Nanotech. **15**, 833 (2004)

X-ray LWFA in a tube vs. uniform solid

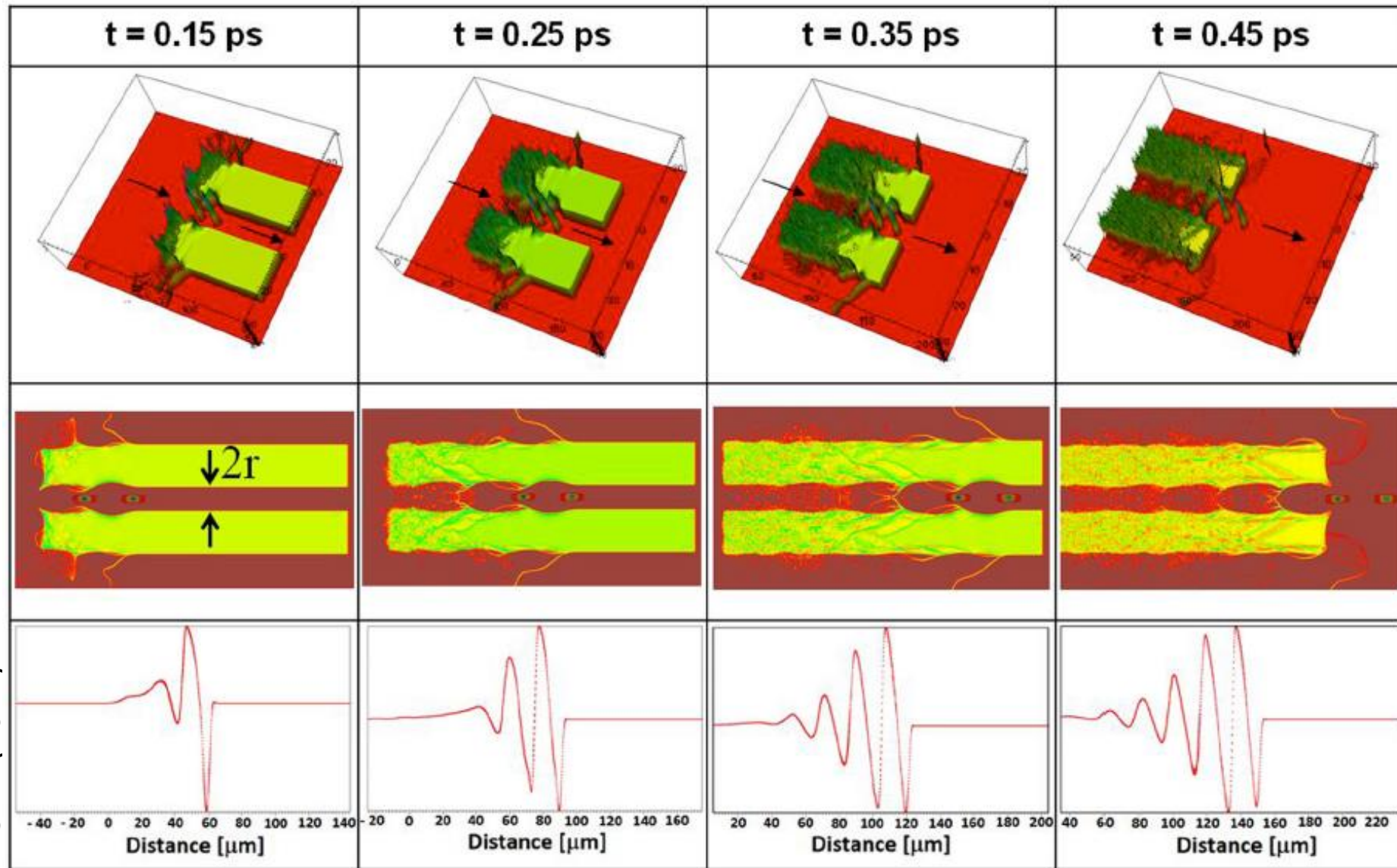


in nanotube

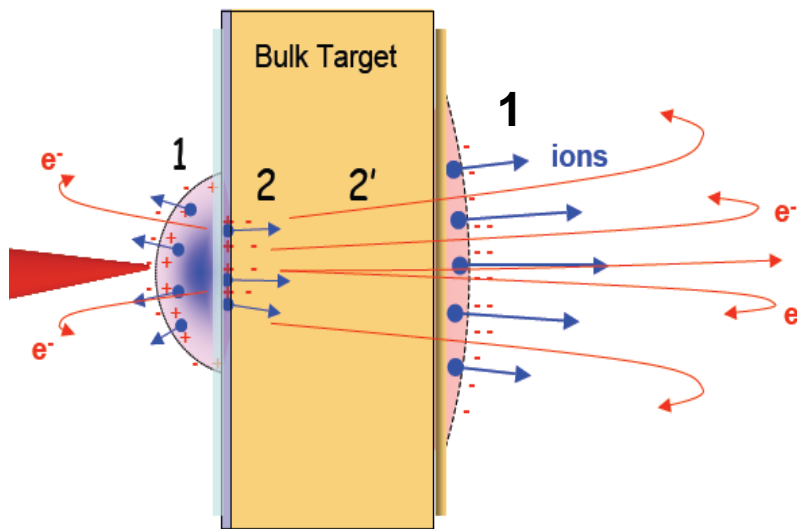
in uniform solid

A few-cycled 1keV **X-ray pulse** ($a_0 \sim O(1)$), causing 10TeV/m wakefield in the tube
more strongly confined in the tube
cf: uniform solid

Beam-driven wakefield on a chip



Laser-driven ion acceleration mechanisms



$$E \sim TV/m$$

1)TNSA

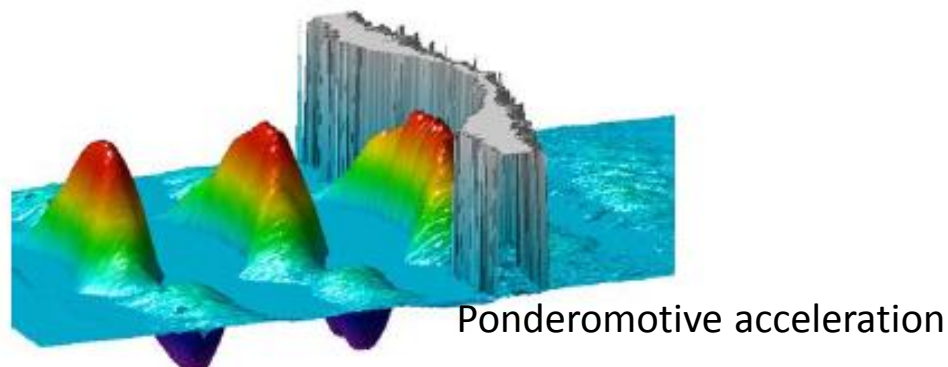
micron thick targets

incoherent process

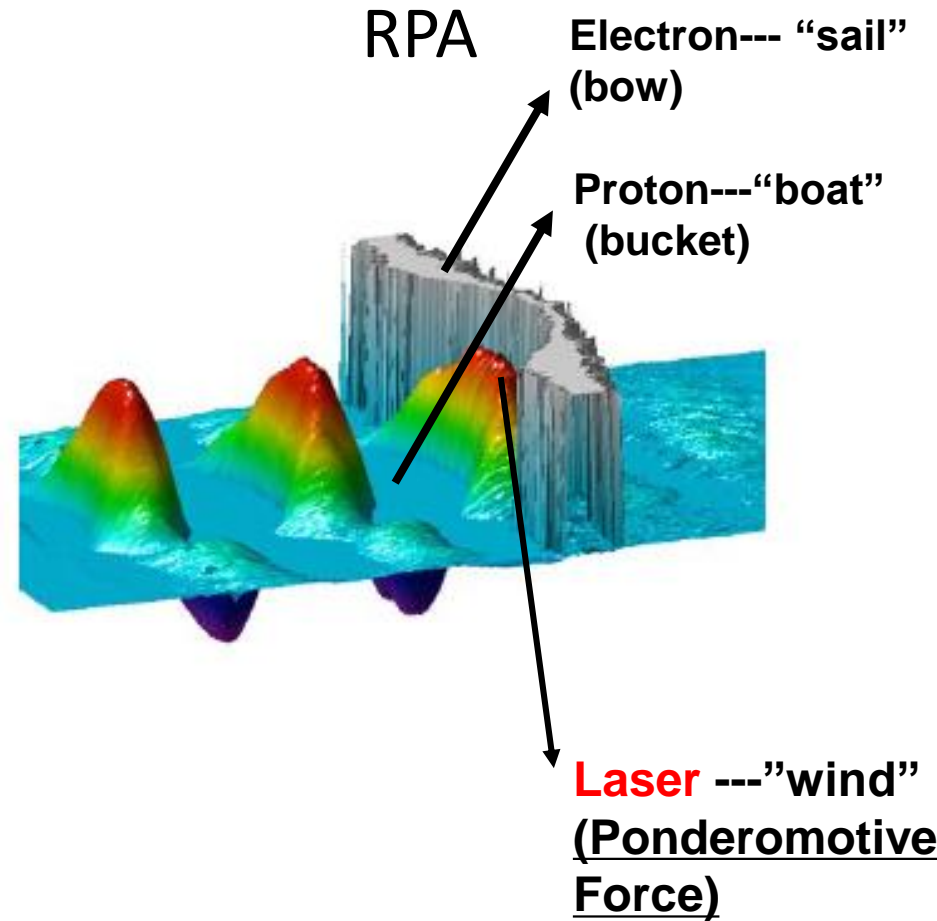
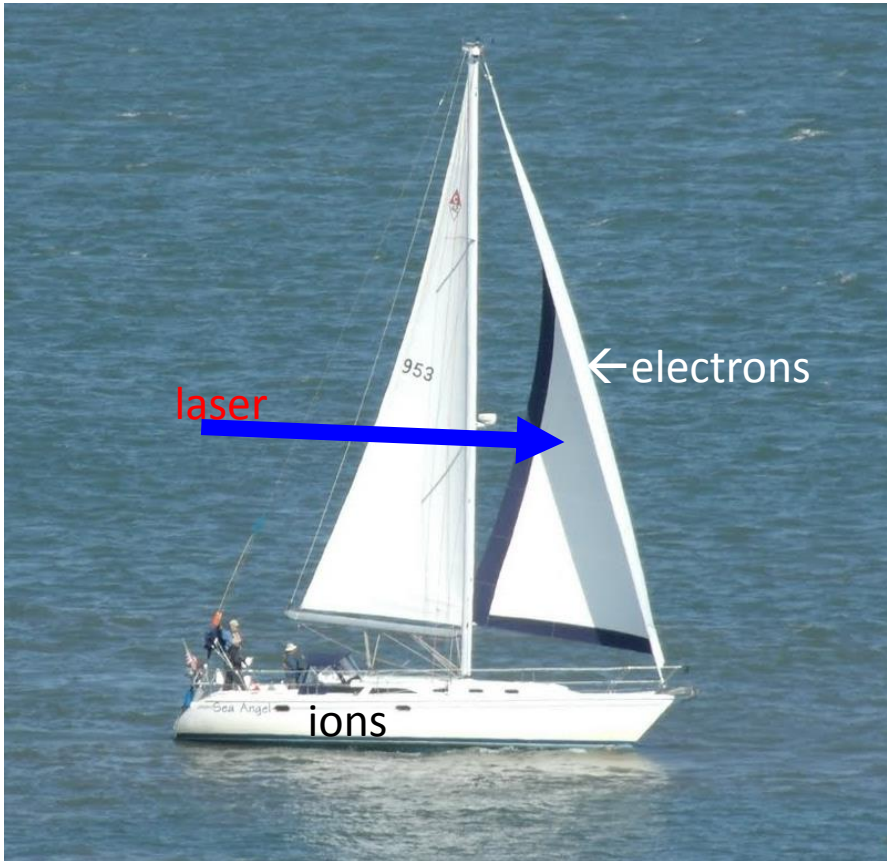
2)RPA

nanotargets

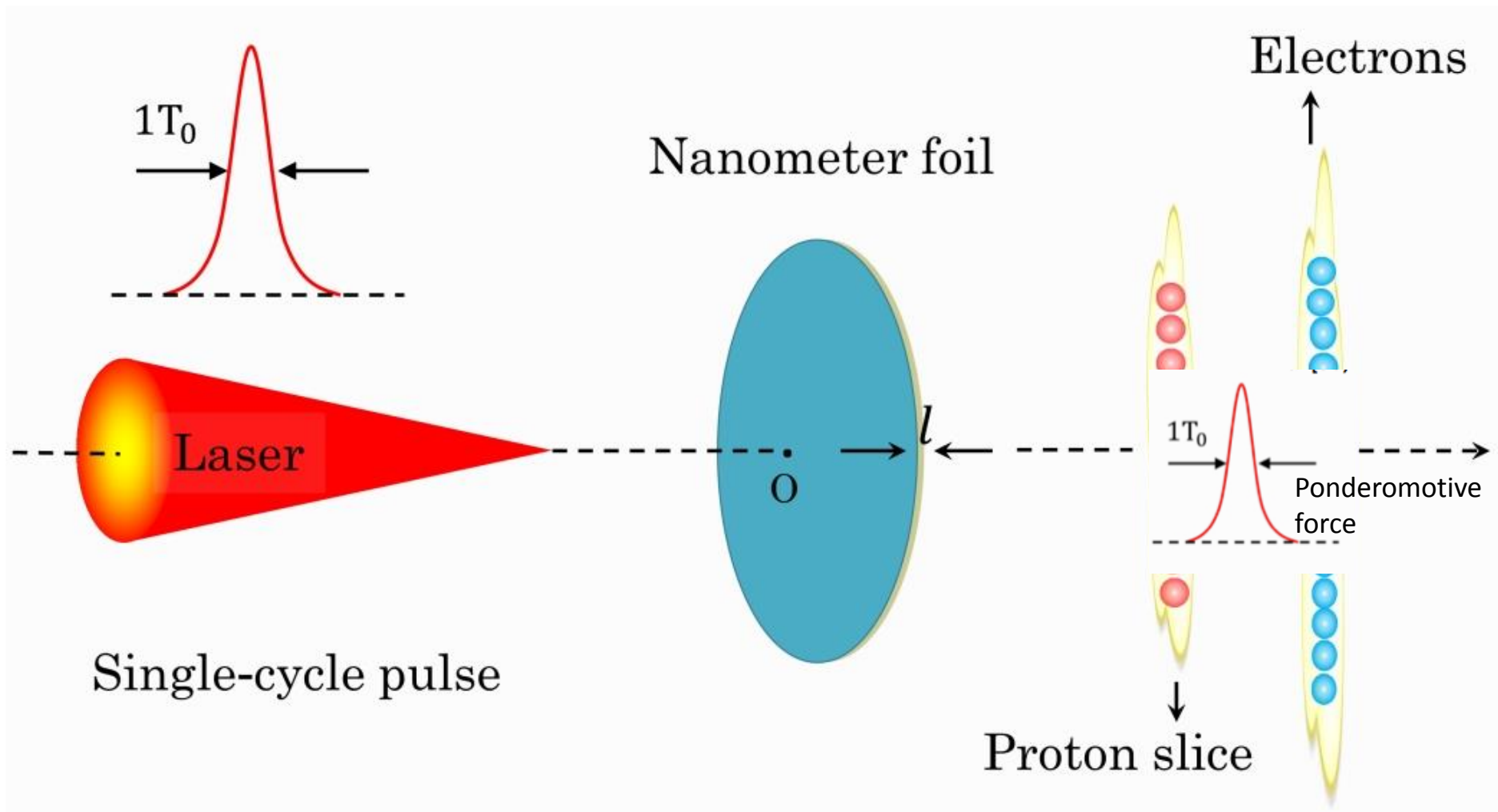
can be coherent



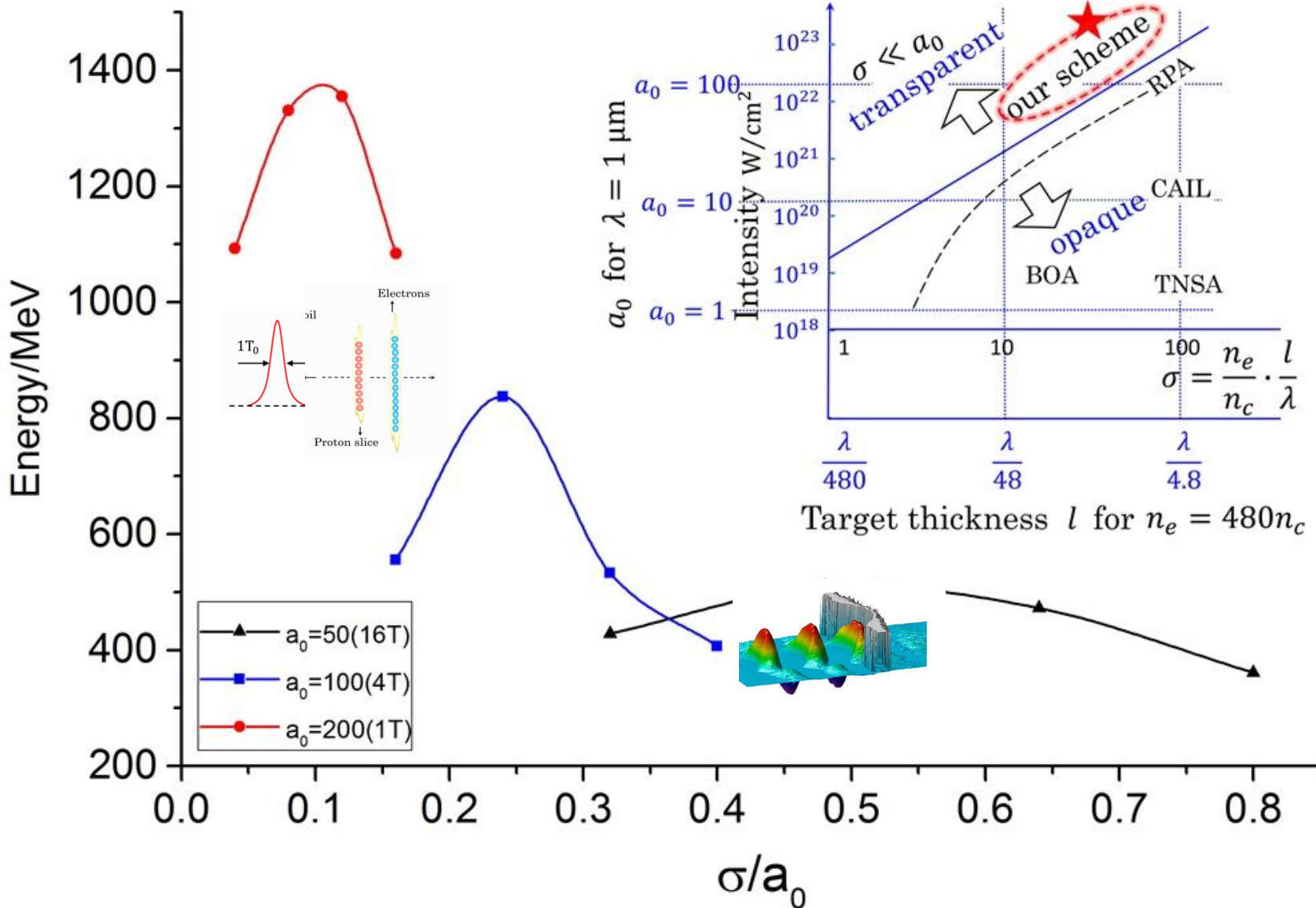
RPA (Radiation Pressure Acceleration)

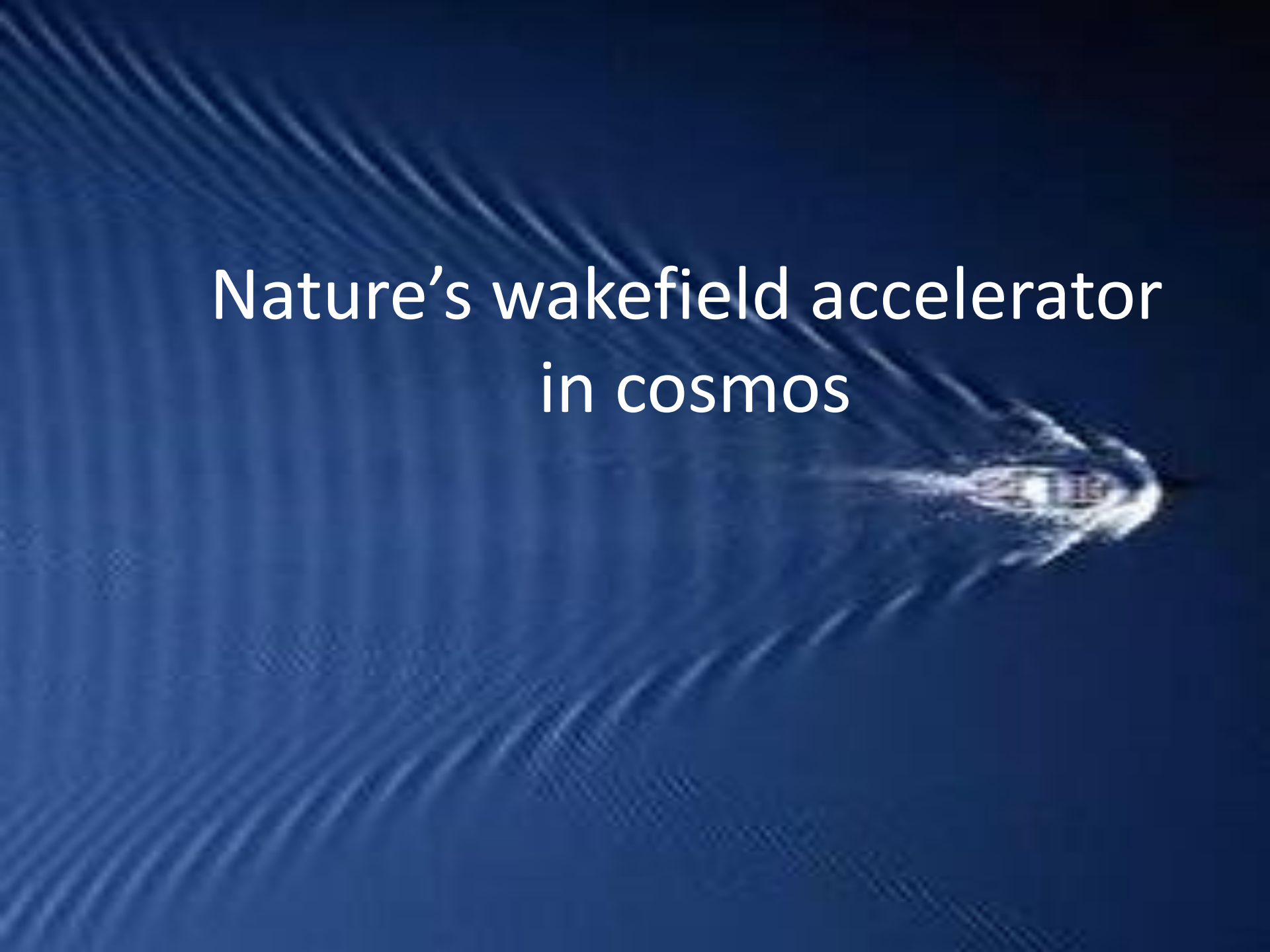


single-cycle pulse ion acceleration regime



Laser-driven ion acceleration: TNSA, RPA and our regime





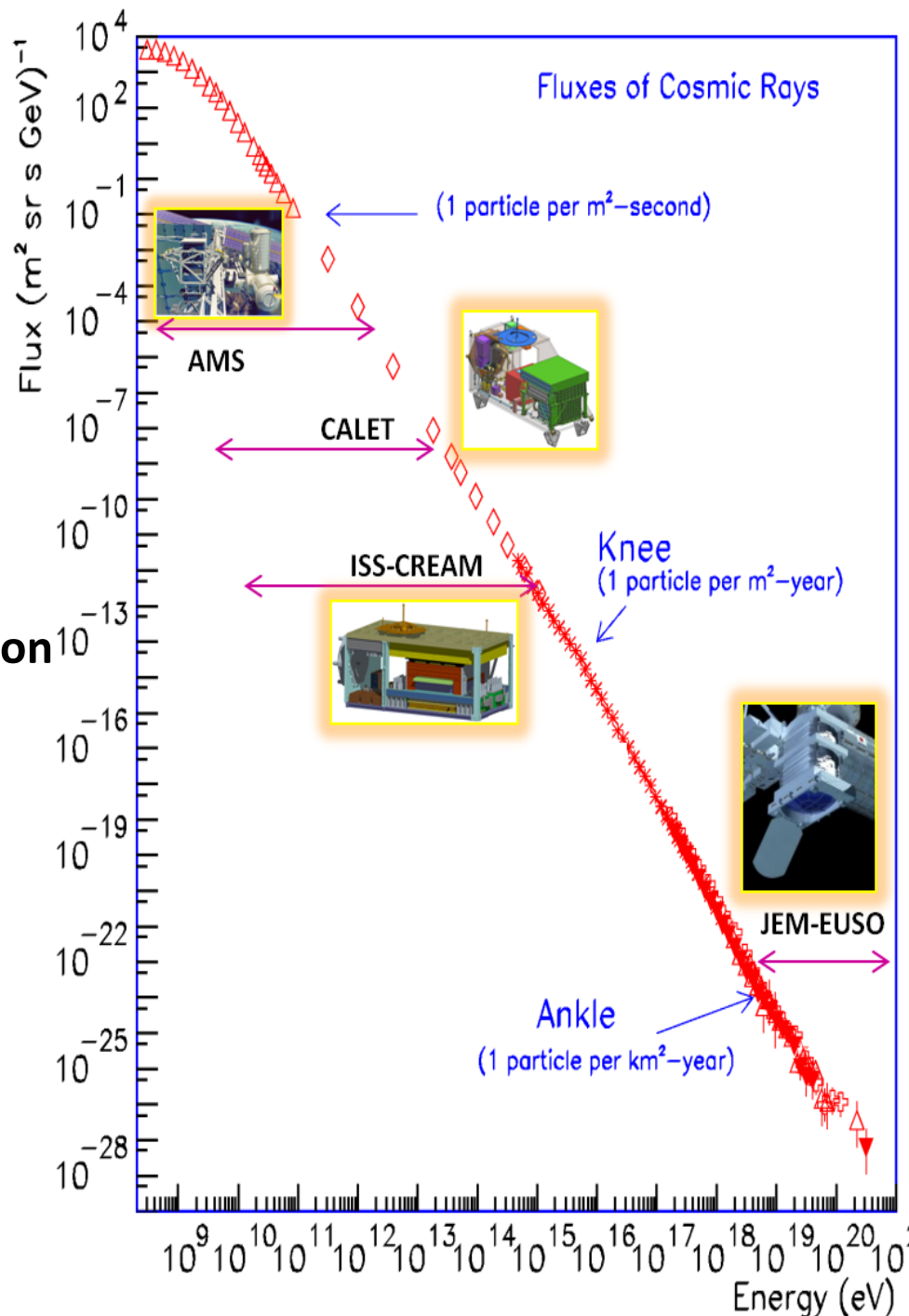
Nature's wakefield accelerator
in cosmos

Ultrahigh Energy Cosmic Rays (UHECR)

Fermi mechanism runs out of steam
beyond 10^{19} eV
due to synchrotron radiation

Wakefield acceleration

comes in rescue
prompt, intense, linear acceleration
small synchrotron radiation
radiation damping effects?

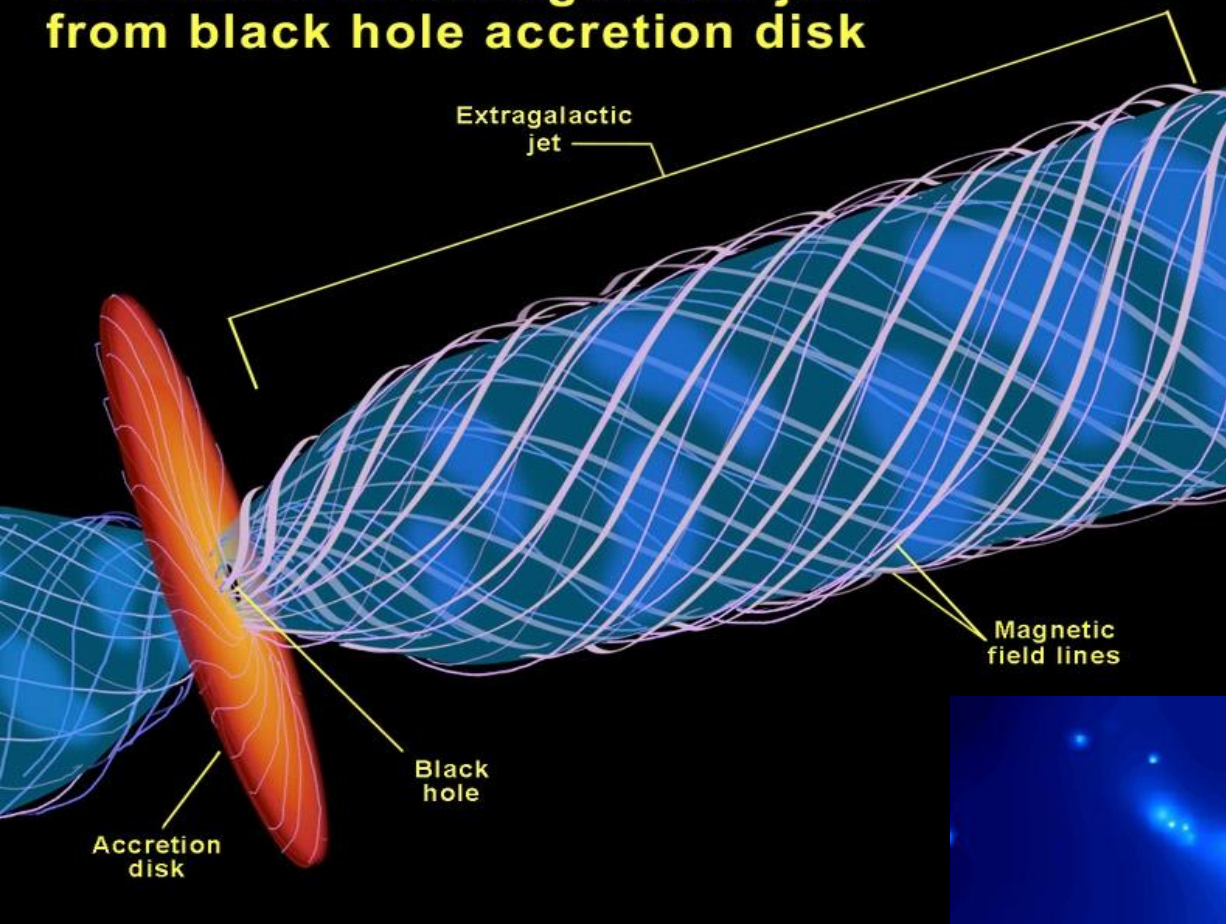


Cen A



- Distance : 3.4Mpc
- Radio Galaxy
 - Nearest
 - Brightest radio source
- Elliptical Galaxy
- Black hole at the center w/
relativistic jets

Formation of extragalactic jets from black hole accretion disk



Fermi's 'Stochastic Acceleration'
(large synchrotron radiation loss)



Coherent wakefield acceleration
(no limitation of the energy)

Nature's LWFA : Blazar jets

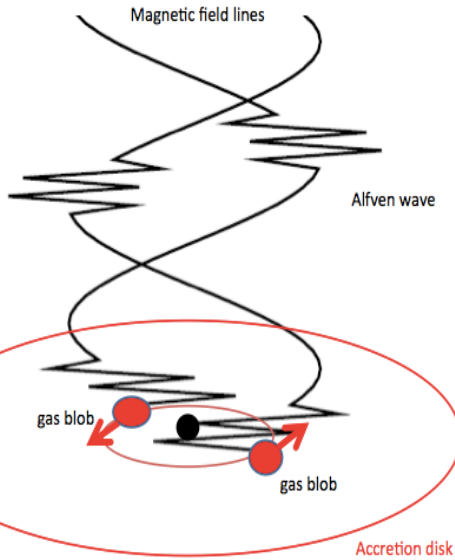
extreme high energy cosmic rays ($\sim 10^{21}$ eV)

episodic γ -ray bursts observed

consistent with LWFA theory



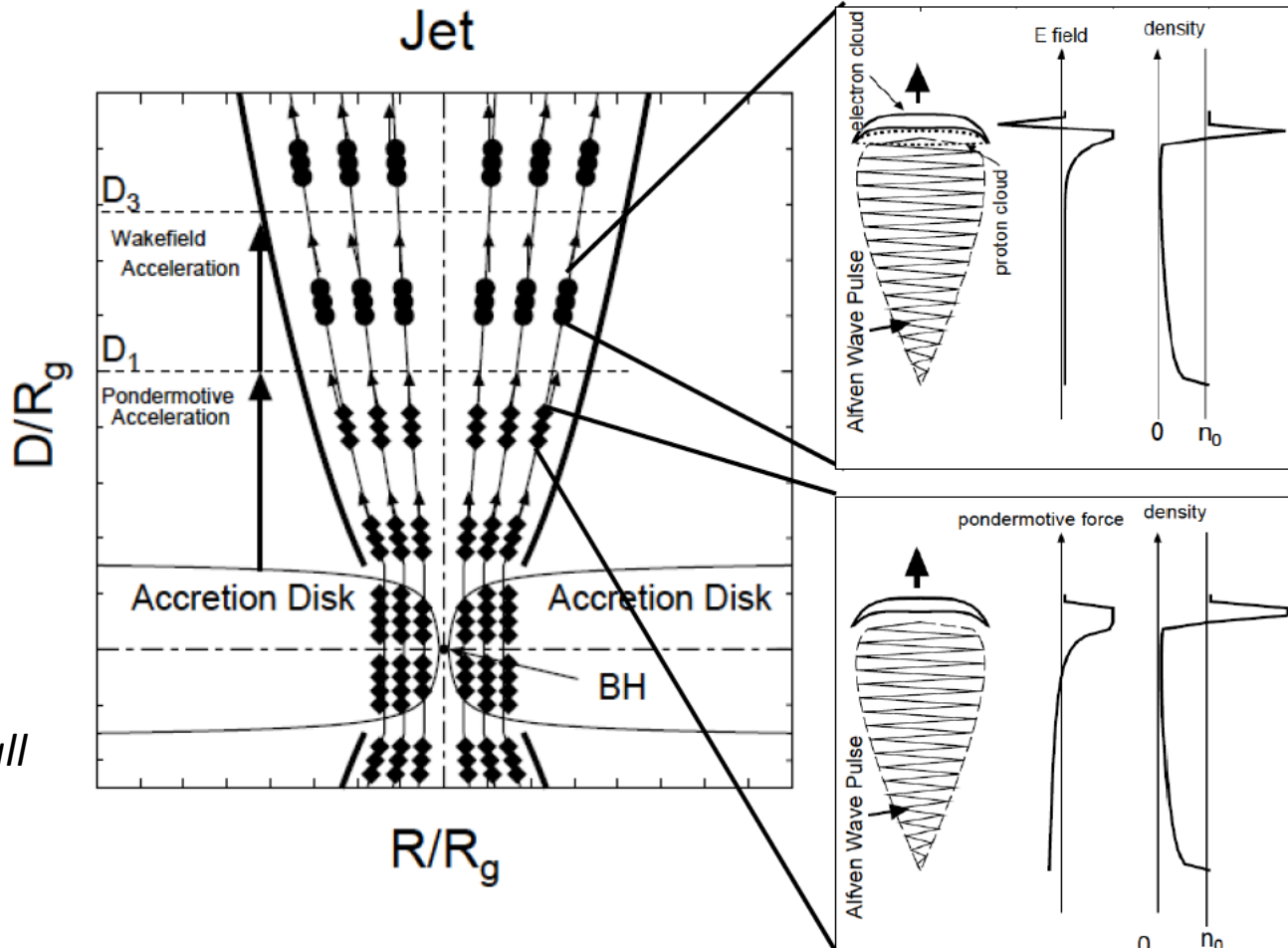
Astrophysical wakefield acceleration: Superintense Alfvén Shock in the Blackhole Accretion Disk toward ZeV Cosmic Rays ($a_0 \sim 10^6$ - 10^{10} , large spatial scale)



$$a_0 = eE_0 / mc\omega_0 \gg 1$$

E_0 : modest

ω_0 : extremely small



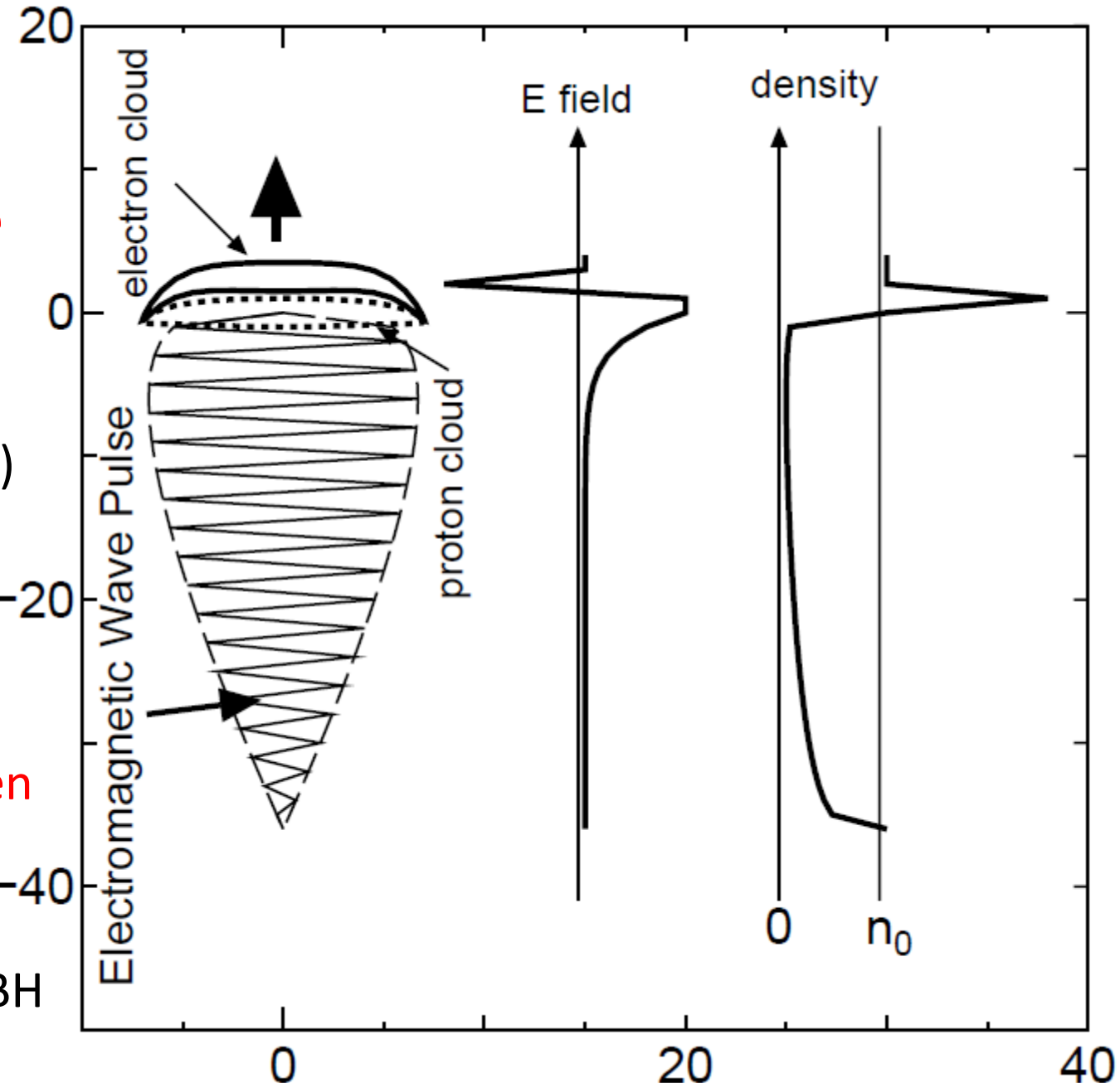
Wakefield vs. Ponderomotive Acceleration

wavebreak (1D or 2D)

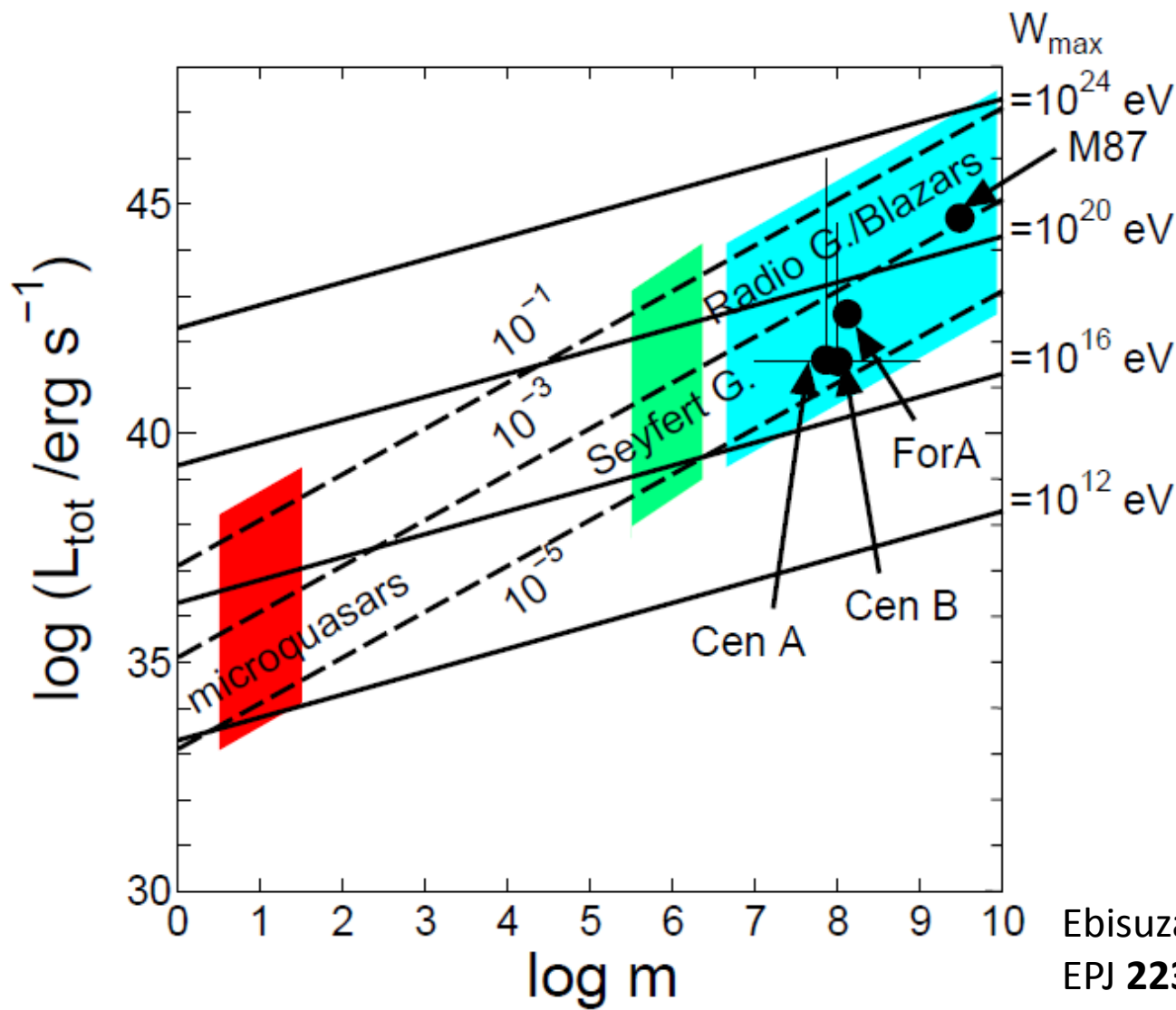
in higher a_0
 \rightarrow wakefield
 less important

Ponderomotive-driven
 Acceleration more
 robust ($a_0 \gg 1$)

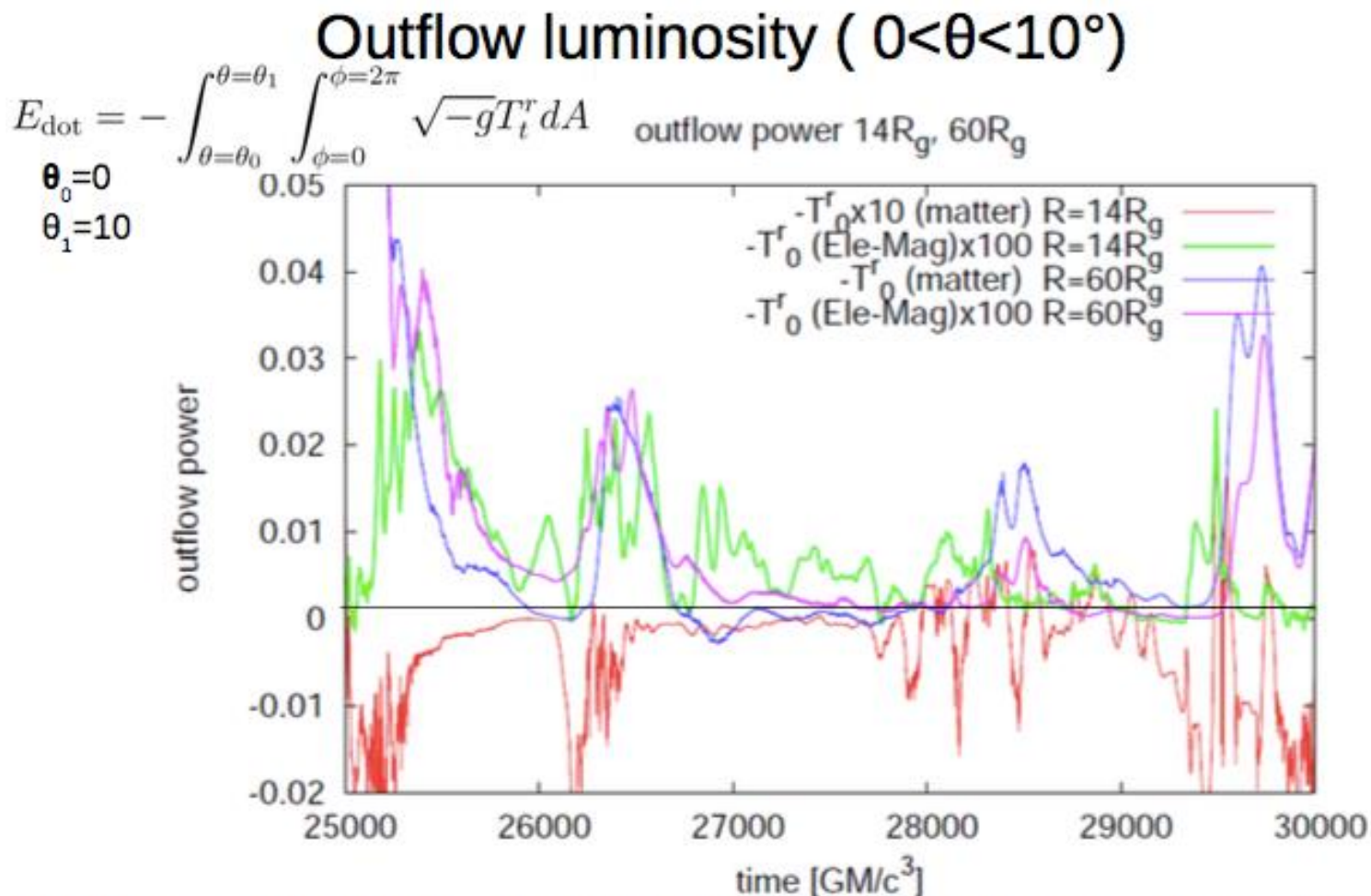
$a_0 \sim 10^{6-10}$ in AGN BH



Comic ray acceleration and γ -ray emission: Summary



General Relativistic MHD simulation of accretion disk + jets

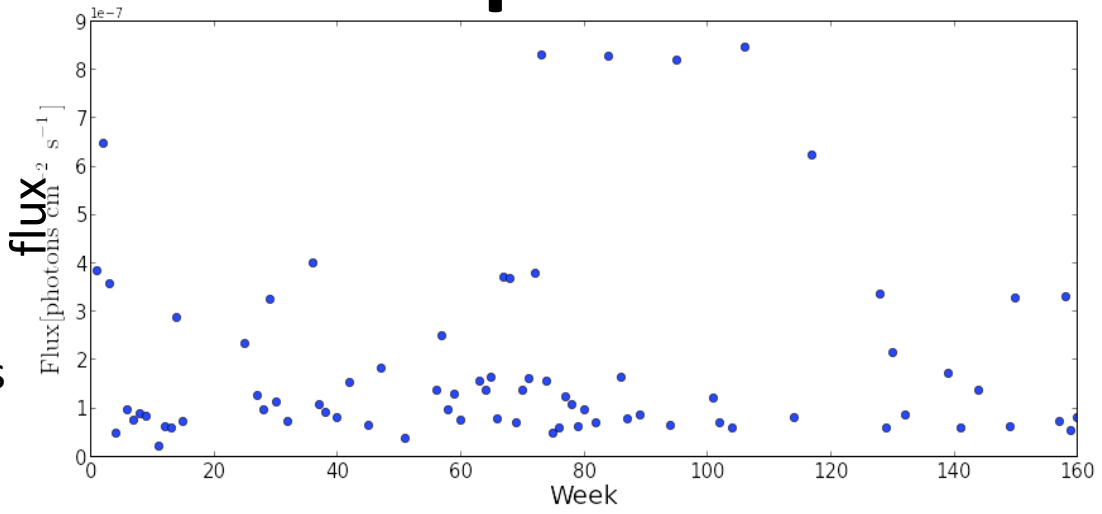


Short time variability ($\Delta t \sim$ a few tens GM/c^3) in electromagnetic components (green and pink) : Good agreement with Ebisuzaki & Tajima(2014) $t_{var} \sim M$ => possible origine for flares in blazars,
strong Alfvén wave mode => Application to wake field acc. for UHECRs

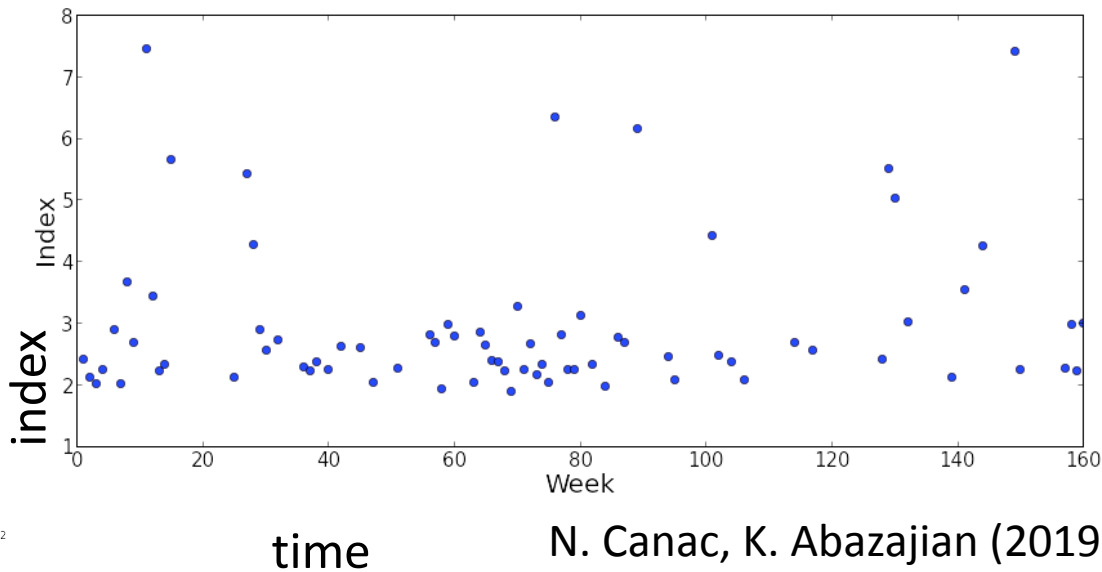
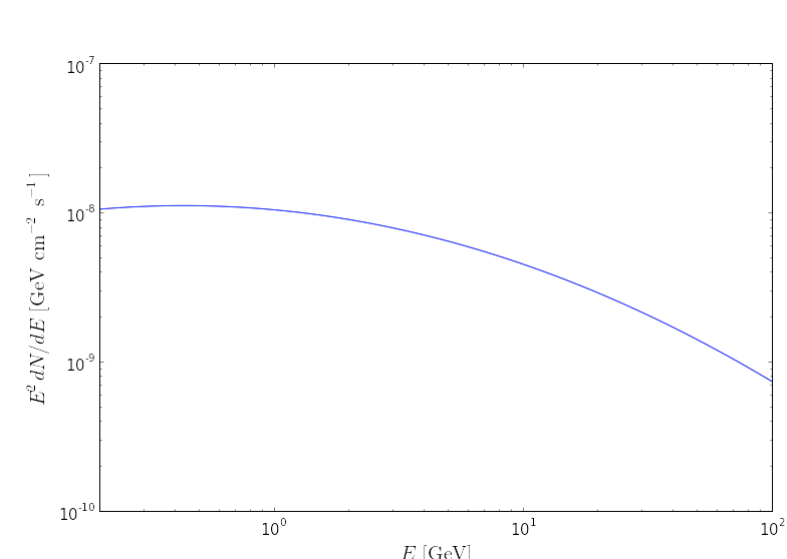
Blazar shows anti-correlation between γ burst flux and spectral index

Blazar: AO0235+164
 $M \sim 10^8 M_{\text{Sun}}$

Rise time < week (less than a unit),
Period between bursts ~ 10 weeks
Spectral index $\Rightarrow 2$
(~ Ebisuzaki/Tajima theory)



→ all quantitatively consistent with Wakefield theory



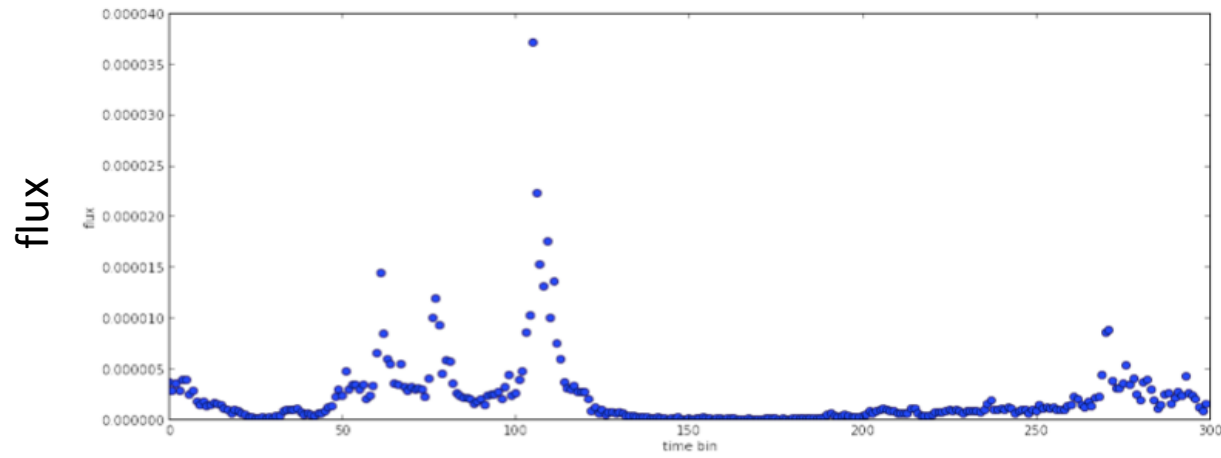
time

N. Canac, K. Abazajian (2019)

Again, Anti-correlation even in a bigger blazar

Blazar: 3C454.3

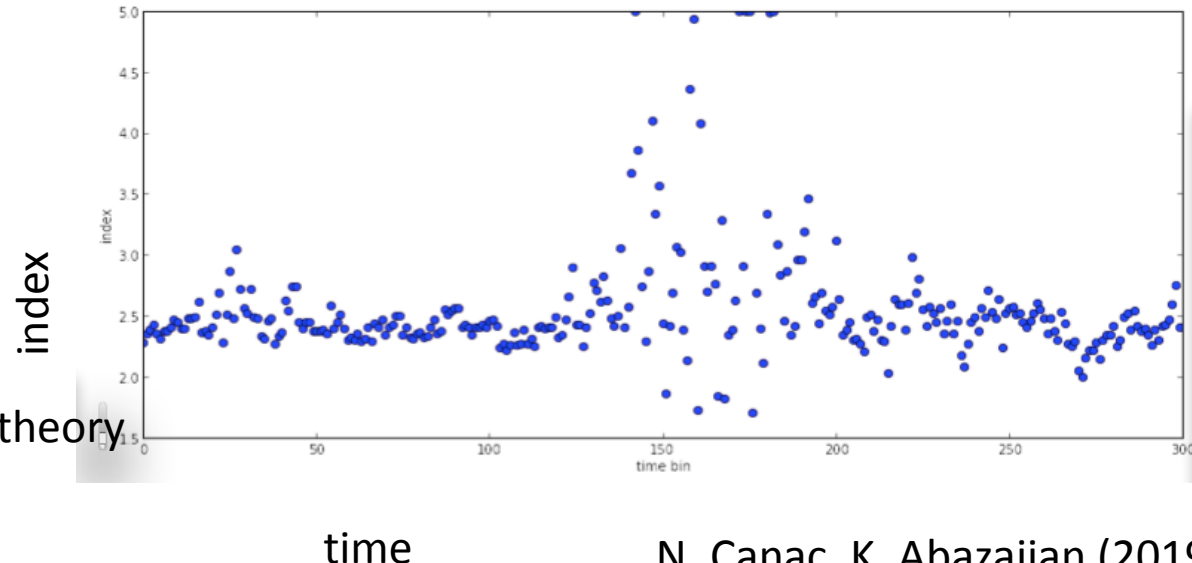
$M \sim 10^9 M_{\text{Sun}}$



Same anti-correlation as
AO0235+164

The rise time and burst periods
a lot longer (by an order of
magnitude)

Quantitative agreement and
correct scaling with Blazar mass
with (broader sense of) Wakefield theory
(Ebisuzaki/Tajima)
period $\sim M$; luminosity $\sim M$

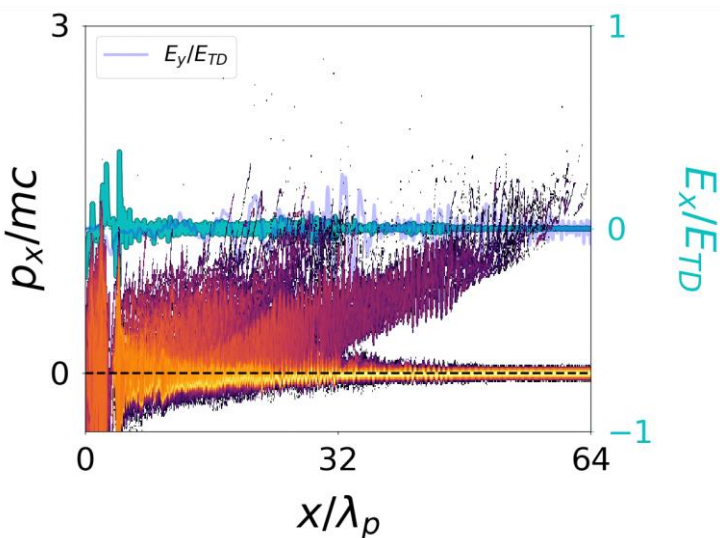


time

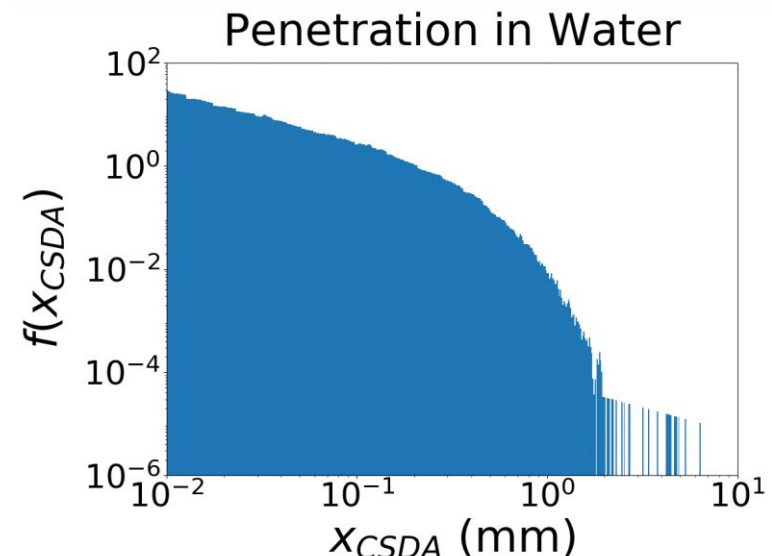
N. Canac, K. Abazajian (2019)

High density **wakefields** for medicine

- Micron accelerator in endoscope by **fiber laser**
- Density $\sim 10^{21} \text{ cm}^{-3}$ nanomaterials target
- Theranostics



Critical density wakefield acceleration



Conclusions

- Demonstrated: ultrafast pulses, coherent collective (robust) **wakefield** (GeV/cm) excitable.
- Thin-Film Compression (TFC)
- Single-cycled **laser** → single-cycled **X-ray laser**
- Wakefield in nanostructure (TeV/cm): accessible
- **Wakefield** acceleration: Nature's accelerators favored for EHECR, **gamma ray** bursts from Blazars
- Applications: **LWFA** endoscopic radiation therapy (ESRT) $\leftarrow \mu\text{m}$ accelerator \leftarrow fiber **laser**



A 3D molecular model of a protein-DNA complex. The protein is shown as a red ribbon structure, and the DNA is represented by a helical arrangement of colored sticks (red, green, blue). A central cavity contains several large, semi-transparent spheres in purple, green, and blue. Small white spheres representing water molecules are scattered throughout the scene.

Thank you!